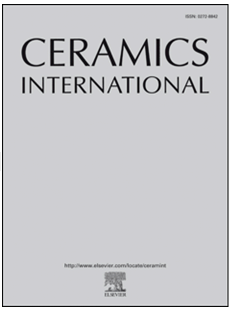

Silica nanoparticles self-assembly process in polymer composites: Towards advanced materials

Barbara Di Credico, Elisa Manzini, Lorenzo Viganò, Carmen Canevali, Massimiliano D'Arienzo, Silvia Mostoni, Roberto Nisticò, Roberto Scotti

PII: S0272-8842(23)01384-6

DOI: https://doi.org/10.1016/j.ceramint.2023.05.125

Reference: CERI 36654

To appear in: *Ceramics International*

Received Date: 13 March 2023

Accepted Date: 14 May 2023

Please cite this article as: B. Di Credico, E. Manzini, L. Viganò, C. Canevali, M. D'Arienzo, S. Mostoni, R. Nisticò, R. Scotti, Silica nanoparticles self-assembly process in polymer composites: Towards advanced materials, *Ceramics International* (2023), doi: https://doi.org/10.1016/j.ceramint.2023.05.125.

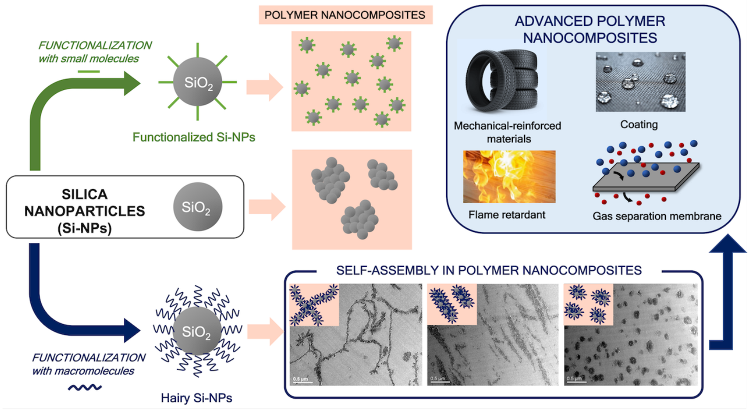
POLYMER NANOCOMPOSITES
ADVANCED POLYMER NANOCOMPOSITES
FUNCTIONALIZATION with small molecules
SiO_2
Functionalized Si-NPs
Mechanical-reinforced materials
Coating
SILICA NANOPARTICLES (Si-NPs)
SiO_2
Flame retardant
Gas separation membrane
SELF-ASSEMBLY IN POLYMER NANOCOMPOSITES
SiO_2
FUNCTIONALIZATION with macromolecules
Hairy Si-NPs

Silica nanoparticles self-assembly process in polymer composites: towards advanced materials

Barbara Di Credico,[1] Elisa Manzini,[1] Lorenzo Viganò, Carmen Canevali, Massimiliano D'Arienzo, Silvia Mostoni, Roberto Nisticò and Roberto Scotti*

Dept. of Materials Science, INSTM, University of Milano-Bicocca, Via R. Cozzi, 55, 20125Milano, Italy. Tel: +39-02-64485189; e-mail: barbara.dicredico@unimib.it

[1] These authors contributed equally to this work.

Abstract

The incorporation of silica nanoparticles (Si-NPs) into the polymer matrix is a growing area of interest research to produce high-performance polymer nanocomposites (NCs) across a wide range of nanotechnology applications. This improvement is due to the Si-NPs capability to self-assembly giving rise to specific well-organized structures with both short- and long-range order across a hierarchy of spatial scales, determined by both NP-NP and NP-matrix interactions, involving a careful balance among attractive driving forces, repulsive forces, and directional forces.

Respect to this, the aim of the present paper is to systematically review the use of Si-NPs in polymer NCs and on the role of NPs self-assembly in determining the final material properties.

Firstly, we explored the synthesis and modification of both isotropic and anisotropic Si-NPs in relation with use in NC materials, focusing on NPs dispersion and distribution, as well as on the functionalization strategies of Si-NPs. Besides Si-NPs functionalization with conventional small organic molecules, a large section is devoted to an emerging class of functionalized Si-NPs with macromolecules, namely silica hairy NPs (Si-HNPs), able to give rise a a rich variety of complex assemblies and materials with new structures and functionalities. Successively, NCs materials containing Si-NPs and Si-HNPs have been explored in terms of synthetic preparation and properties. The self-organization of Si-NPs and Si-HNPs in polymer matrices has been reported and its effect on the functional materials properties have been evaluated with a critical point of view on the results, limits, and future perspectives.

Our review can be considered a tutorial work, aiming at providing useful insights to researchers in the field of nanotechnology and nanoscience, taking into consideration the fundamental role of NPs self-assembly processes in determining the functional material properties.

Keywords: silica, nanocomposites, self-assembly nanoparticles

1. Introduction

The process of self-organization or self-assembly universally occurs in non-equilibrium systems belonging to living matter, geochemical environments, materials science and industry. In materials science, self-assembly is the association process of individual building block units of a given material of any size (from small molecules to particles) into highly ordered structures, ranging from angstroms to centimetres with different sizes and shapes [1]. In self-assembly processes, the interactions between the building blocks are non-covalent but mainly based on hydrophobic, electrostatic, van der Waals forces, hydrogen bonding, π-π aromatic stacking and metal coordination. Despite their weakness (2–250 kJ/mol), these interactions give rise to stable organized structures, determining the shape, size, and functionality.

Nanoparticles (NPs) self-assembly plays an important role across a wide range of nanotechnology applications [2–4]. NPs are able to interact with each other giving rise to specific well-organized structures with both short- and long-range order across a hierarchy of spatial scales. This organization takes place in materials consisting exclusively of NPs or, alternatively, materials in which the NPs are dispersed within a polymeric medium [5,6]. In the latter case, when inorganic nanoscale building blocks are dispersed within polymers, the spontaneous assembly of NPs into highly organised structures is determined by both NP-NP and NP-matrix interactions, involving a careful balance among attractive driving forces, repulsive forces, and directional forces. Overall, the preparation of the nanocomposite (NC) materials by specifically localizing and orienting the NPs appears highly promising, paving the way to novel families of materials offering extraordinary property improvements. In fact, although the complete filler dispersion in a polymeric matrix is challenging to maximize the interfacial area[7], on the other hand, it is well clarified that the creation of a filler network, i.e. fractal organizations of filler NPs in a polymer matrix, is fundamental to obtain critical properties. This requires the modification of the NPs surface chemistry in order to control their interactions both with themselves and, at the interface with the polymer, allowing to obtain desired properties or applications.

Among NPs, silica NPs (Si-NPs) have been extensively used in materials applications due to their low cost of fabrication, availability, and ability to modify their surface properties [8]. The preparation, characterization, properties, and applications of polymer/silica NCs have become a quickly expanding research field, as testified by several books and review articles appeared in the last decades [9]. Besides, the impact of Si-NPs on materials properties has been increasingly associated with their capability to originate interesting and organized structures by means of self-assembly processes [10]. Since this subject has not yet been systematically reviewed, the purpose of this review is to give a rationale for the use of Si-NPs in polymer NCs and on the role of NPs self-assembly in determining the final material properties.

This review article is organized as follows. Section 2 reports the synthesis and modification of both isotropic and anisotropic Si-NPs, focusing on their use in NC materials. In fact, the possibility of designing advanced hybrid materials based on NPs requires the development of new protocols for both particle synthesis and surface-functionalization. In this contest, an overview on NPs dispersion and distribution, as well as on the functionalization strategies of Si-NPs with conventional small organic molecules, such as silanes, are herein presented. Section 3 is devoted to Si-NPs functionalization with macromolecules, which gives rise to an emerging class of functionalized Si-NPs, the so-called hairy NPs (HNPs), paving the way for the development of a rich variety of complex assemblies and materials with new structures and functionalities. NCs materials containing Si-NPs are described in Section 4, while the self-organization of Si-NPs and Si-HNPs in polymer matrices and their effect on the functional materials properties are the subjects of Section 5. Finally, Section 6 consists of summaries and perspectives of Si-NPs based materials.

2. Silica Nanoparticles: synthetic strategies and chemical properties

2.1 Synthesis of spherical Si-NPs with defined morphology and surface properties

Silicon oxide, also known as silica, refers to a vast number of chemical species having SiO_2 as chemical formula or $SiO_2 \cdot nH_2O$, if hydrated, which are the most abundant materials of earth's crust.

Silica is composed of tetrahedral units [SiO_4]$^{4-}$, where a silicon ion is at the unit centre and the four oxygen atoms are at the corners of a regular tetrahedron. The solid material is constituted of a network of [SiO_4]$^{4-}$ tetrahedral units linked by Si-O-Si bonds [11]. Depending on the distribution of tetrahedral units, two different forms of silica can be detected: crystalline and amorphous.

In nature, SiO_2 mainly exists in the crystalline form, with smaller surface area and health-damaging problems. Furthermore, mineral silicas, despite being widely available in nature, are difficult to process and highly contaminated by several metal ions [12]. Therefore, for scientific and industrial applications, amorphous silica produced by chemical synthesis is largely preferred.

The most common synthetic approaches for silica can be divided into two main classes, defined by the phase of the silica precursor: gaseous or liquid.

Amongst the gaseous synthetic approaches, arc discharge methods have been abandoned due to their extremely high-energy requirement, whereas fumed silica is still employed in many technological applications. Pyrogenic or fumed silica is produced through a chemical vapour condensation (CVC) method, which consists of the vaporization and polymerization of silicon tetrachloride, $SiCl_4$, in a hydrogen and oxygen flame at temperature between 1100 and 1800 °C (Eq. 1) [13].

$$2H_{2(g)} \; + \; O_{2(g)} \; + \; SiCl_{4(g)} \xrightarrow{>1000\,°C} SiO_{2(s)} \; + \; 4HCl_{(g)} \qquad (Eq.\ 1)$$

The product consists of non-porous silica primary particles with a diameter between 5 and 50 nm that, due to the high temperature required, form aggregates of anhydrous mesoporous silica with high specific surface area (50-400 m^2/g) and low concentration of surface silanols. The advantage of this approach is that $SiCl_4$ is a toxic by-product of the polysilicon industry, hence it is cheap and available, but the high energy required makes this synthetic method expensive [12].

For this reason, due to the current attention toward energy and environmental impact, the research activity has shifted its focus on liquid silica synthetic methods. The most common silica employed in industrial application is precipitated silica. SiO_2 is produced by the neutralization of an aqueous solution of sodium silicate with sulfuric acid (Eq. 2) to generate silicic acid in a high concentration that induces silica polymerization and precipitation [14].

$$Na_2O \cdot 2.6\, SiO_2 + H_2SO_4 \rightarrow 2.6\, SiO_2 + Na_2SO_4 + H_2O \qquad (Eq.\ 2)$$

By modulating the reaction parameters, such as temperature, reactant concentration and medium, the size of nano-silica can be controlled, whereas the shape remains spherical. Precipitated silica possesses specific surface area in the range of 30-800 m^2/g and primary particles with diameters between 5 nm and 100 nm, but their high aggregation increases the dimension up to microns. More important, precipitated silica presents a large number of silanols, which are fundamental for the chemical surface modification of the NPs. Despite precipitated silica includes large quantities of sulphate and alkaline earth ions as impurities, this synthetic process uses highly available silica precursors and guarantees low environmental impact [12,15].

The Stöber process [16] is the most popular and versatile approach for the synthesis of colloidal Si-NPs because it provides better control over their properties, in particular size, surface chemistry and shape. The molecular precursors involved are silicon alkoxides with general formula $Si(OR)_4$, where R is generally methyl (tetramethylorthosilicate, TMOS) or ethyl (tetraethylorthosilicate, TEOS). The reaction occurs in the presence of ammonia as catalyst and a mixture of ethanol and water as solvent [16]. The Stöber method proceeds with a combination of hydrolysis and condensation reactions of the alkoxysilane. The hydrolysis step causes the conversion of alkoxy groups into silanol groups via the nucleophilic attack of water. The second step, the condensation, consists in the polymerization of Si-OH and Si-OR groups to create siloxane bridges (Si-O-Si), typical of the silica structure (Eq.s 3-5) [17].

$$\mathrm{Si(OR)_4 + xH_2O \xrightarrow{hydrolysis} Si(OR)_{4-x}(OH)_x + xROH} \qquad (Eq.\ 3)$$

$$\mathrm{(OR)_3Si-OH + HO-Si(OR)_3 \xrightarrow{water\ condensation} (OR)_3\,Si-O-Si(OR)_3 + H_2O} \qquad (Eq.\ 4)$$

$$\mathrm{(OR)_3Si-OR + HO-Si(OR)_3 \xrightarrow{alcohol\ condensation} (OR)_3\,Si-O-Si(OR)_3 + ROH} \qquad (Eq.\ 5)$$

By controlling the experimental conditions, such as the chemical structures of both alcohols and precursors, the relative concentrations of the reagents, the reaction temperature and the feed rate of reactants, highly monodispersed silica nanospheres with sizes ranging from 5 to 2000 nm have been produced [18]. On the other hand, the higher cost of alkoxysilane reactants, compared to sodium silicate, and the requirement of basic conditions and organic solvents make this method not suitable for large-scale production of silica.

2.2 Synthesis of shape-controlled anisotropic Si-NPs

The preparation of anisotropic Si-NPs is not an easy task because the commonly applied synthesis methods for silica provide spherical or slightly irregular particles. The electrospinning process is a relatively simple, inexpensive, and scalable strategy for obtaining shape-controlled nanomaterials. By applying this method, a solution of the precursor, generally TEOS, is mixed with an alcoholic solution of polyvinylpyrrolidone (PVP) and loaded into a capillary connected to a high-voltage source. The deposition of silica on the target of the device provides the material in the form of nanofibers [19] or nanowires (Figure 1) [20]. As an alternative, nano-silica can be produced with the chemical vapour deposition (CVD) technique. The process requires the condensation of a precursor, generally TEOS, SiH_4 or $SiCl_4$, from the gas phase on a heated substrate, in a vacuum chamber. On the support, the reaction or the thermal decomposition of the precursor induces Si-NPs formation; the reaction can be initiated by thermally heating the substrate or applying a plasma [21]. This technique was used for the production of uniform and pure Si-NPs, such as nanowires [22] or nanosprings [23], but the required high temperature (-1000 °C for thermal heating, 300-700 °C for plasma) and low pressure implies (from 2-3 Torr to less than 10^{-8} Torr) a high energy cost.

The most versatile strategy to produce shape-controlled Si-NPs consists in the synthesis of silica nanoparticles on anisotropic structures and the following removal of the template, solely by calcination and acid or base etching, allows to obtain the replica.

A good method to perform templated assembly involves the use of a hard template, namely a pre-synthesised anisotropic NP. By a sol-gel procedure, the template can be coated with silica to produce hollow or core-shell nanostructures, producing different silica structures, such as nanoshells, nanotubes, nanocubes, and nanorods, by using gold nanorods [24], $CaCO_3$ [25], Cu_2O (Figure 1c) [26] or Ni-hydrazine [27] as hard templates.

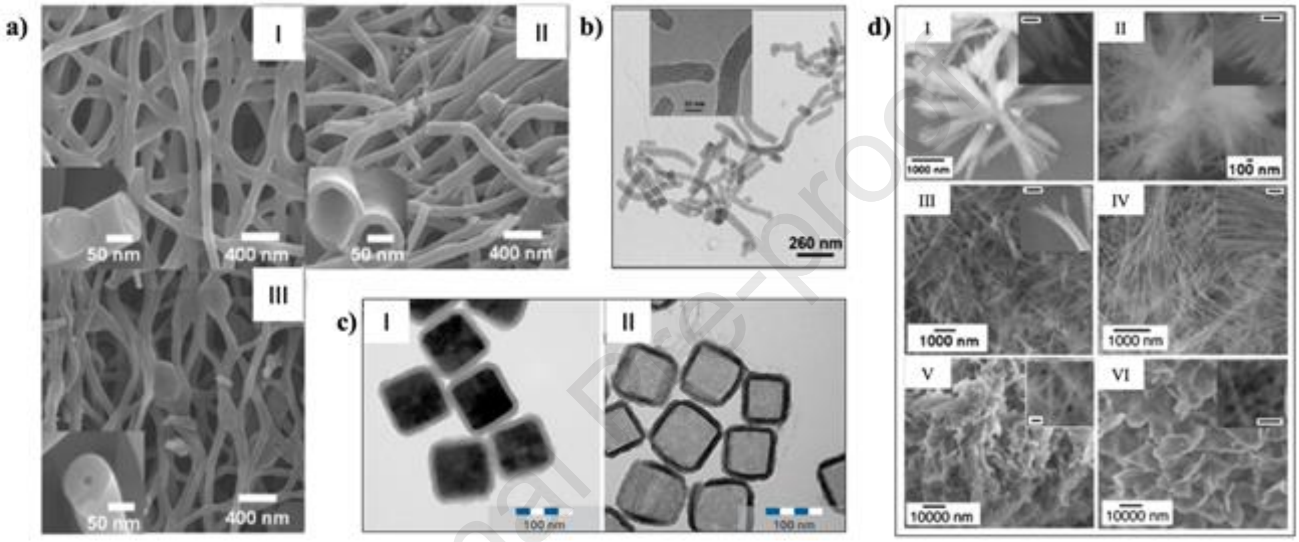

Figure 1. Different types of anisotropic Si-NPs: a) SEM images of silica nanowires obtained by electrospinning of a TEOS solution mixed with a PVP solution in ethanol: distance collector-syringe 5.5 cm, feeding rate 0.04 ml/h (I) or 0.02 ml/h (II, III) and voltage 10 kV (I) or 8 kV (II, III) [20]; b) TEM images of silica nanorod synthesised by a mixture of TEOS/MPTMS in the presence of CTAB micelles [28]; c) TEM images of $Cu_2O@SiO_2$ core-shell particles (I) and SiO_2 hollow nanocubes after acidic etching of the core (II) [26]; d) SEM images of different shaped silica obtained with a biomimetic process using linear PEI chains: star-shaped (I, II), sponge shaped (III, IV) and leaf-shaped (V, VI). In the inset, magnification images of a-f with scale bare 100 nm [29]. Reprinted with permission from [20], [26], [28] and [29].

To obtain anisotropic NPs, a hollow anisotropic nanostructure was also employed as a mould into which silica is produced. However, due to the difficult access to hollow NPs, this approach is less common than coating. Few examples are available in literature, where the employment of carbon nanotubes [28] or porous anodic aluminium oxide [29] as templates for silica anisotropic NPs is reported.

The same strategy could be also applied to soft templates, namely emulsions and micelles. Emulsions are stable dispersions containing two immiscible phases, generally oil and water, which form domains usually stabilized by surfactants. As the formation of SiO_2 occurs at the interface of the two phases, this strategy can be used to produce both hollow and solid Si-NPs. Kuijk *et al.* [30] produced silica nanorods using a nanoemulsion of water in pentanol stabilized with sodium citrate and PVP as a template.

Micelles are self-assembled specific supramolecular structures made up of amphiphilic molecules, such as surfactants, that form when the surfactants concentration in solution exceeds the critical micelle concentration. These structures can be applied to synthesise spherical NPs, but their shape can also be modulated by the compositions and blocks of surfactant and by the solution conditions including concentration, pH values, temperature, addition of additives and ionic strength [31]. In this context, Du *et al.* [32] proposed the synthesis of silica anisotropic NPs by condensation of TEOS and 3-mercaptopropyltrimethoxysilane (MPTMS) in an aqueous solution, using cetyltrimethylammonium bromide (CTAB) as surfactant. By modulating the TEOS:MPTMS molar ratio, Scotti *et al.* were able to produce both nanospheres and nanorods/nanowires (Figure 1b) with the same procedure [33].

Comparing these two strategies, the use of a hard template provides better control over Si-NPs shape, as well as uniform morphology and dimension, whereas soft template properties are sensitive to the reaction parameters. On the other hand, soft templates are easily produced and eliminated; hence, the process is suitable to be scaled up. Hard templates are more expensive because they are difficult to produce and their elimination is more complicated, hence the process is more time-consuming [31].

A promising strategy to produce silica structures in mild conditions is the biomimetic sol-gel synthesis, which is inspired by the mechanism applied by certain biological organisms, such as diatoms and sponges. These organisms can synthesize silica rapidly, controlling its structure and morphology using water as solvent, at neutral pH and ambient temperature. To achieve these advantages, biological organisms use silica-inducing and silica-coprecipitating molecules, such as long-chain polyamines, specialised proteins (silaffins or silicateins) and saccharides [34,35]. Different synthetic equivalents of these molecules were introduced but, despite their extreme versatility, in vitro silication has not achieved an optimal control over structural and dimensional properties. Up to now, biomimetic strategies allowed only the synthesis of macro-structured silica with nanometric features. As an example, Jin *et al.* [36] employed linear polyethyleneimine chains (a polyamine) with different architectures to direct silica growth towards star, sponge and leaf -shape structures. As reported in the insets of Figure 1d, all the different structures possess elements in the nanoscale range of dimensions.

2.3 Aggregation, dispersion, and distribution of Si-NPs

The surface chemistry and morphology of silica are crucial issues for polymer NCs because they define the adhesion, adsorption and chemical properties of silica at the NP/polymer interface and, hence, the materials performance. The surface of silica is strongly characterized by the presence of free hydroxyl groups, called silanols, that originate due to the saturation of the tetrahedral configuration of silicon atoms [37]. These reactive groups provide the sites for physical adsorption, easily chemically react with multiple substituents, and are crucial for determining the surface properties of silica, as well as their behaviour when added to a polymer matrix.

Silanol groups have been identified and classified [38] as follows (Figure 2): a) isolated silanols (single silanol groups), b) geminal silanols, c) silanetriol (existence not yet demonstrated but postulated), d) vicinal silanols (silanols close enough to form hydrogen bonds).

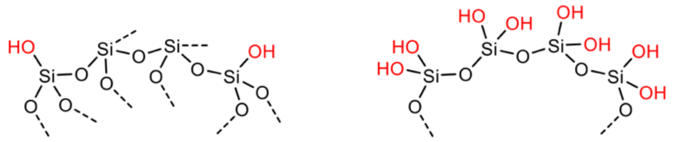

a) Isolated silanols b) Geminal silanols

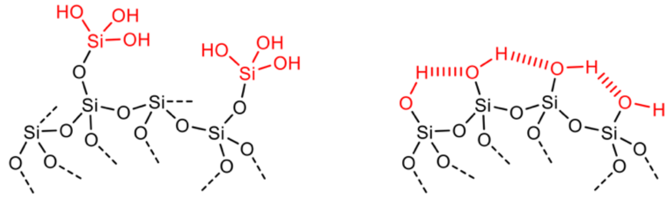

c) Silanetriols d) Vicinal silanols

Figure 2. Schematic representation of the types of silanol groups present on the surface of silica.

The concentration and distribution of silanol groups can be controlled through the synthetic method by changing particles specific surface area, size, porosity, crystallinity and shape [39,40]. In addition, the number of silanol groups changes considerably when silica is thermally treated, indeed, the curing temperature controls the hydration and the hydroxylation degree of the surface [41]. In this context, it is demonstrated that colloidal silica possesses a higher silanols density compared to fumed silica,[42,43] since the latter is synthesized at high temperatures. Furthermore, due to an incomplete hydrolysis of the tetra-alkoxy precursor, Stöber silica surface bears some alkoxy groups, whose number is strictly dependent on the alcohol/water ratio [44].

The presence of a high number of silanol groups on silica surface involves the formation of many hydrogen bonds among the particles. The higher the silanols density and the surface energy, the stronger their interactions and the worse their dispersion. For this reason, Si-NPs are commonly found not as nano-sized primary particles but mainly as aggregates and agglomerates (Figure 3). Agglomerates form as a collection of bounded particles and/or aggregates kept together by Van der Waals forces or physical entanglement. Instead, in the presence of hydrogen bonds or even strong covalent bonds, primary particles form aggregates [45,46].

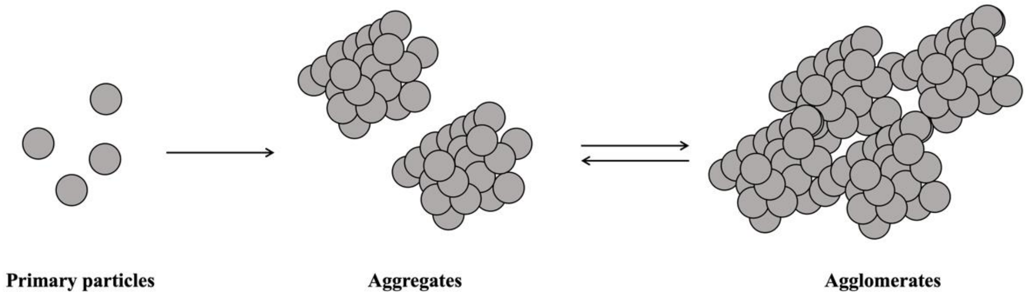

Figure 3. Representation of the formation of agglomerates and aggregates starting from primary silica particles.

Aggregates and agglomerates differ in the stability of their interactions: agglomerates can be easily broken down due to the weaker interactions between particles, on the contrary, aggregates are robust and indivisible [47]. In addition, due to the presence of silanol groups, silica is a highly hydrophilic material; therefore, the material is incompatible with hydrophobic polymers [40].

To control Si-NPs dispersion and aggregation and, hence, improve their distribution in polymer matrices, NPs can be treated with physical and chemical methods. Among physical methods, the high-energy ball milling process and the ultrasonic treatment can be applied. Despite these high-energy processes are useful to break agglomerates, the interactions between aggregates are too strong to break them with conventional mixing facilities [48].

A more efficient strategy is to provide Si-NPs with a steric barrier, functionalizing its surface with organic molecules. This compatibilizer layer has a double function: on one hand, it promotes the dispersion of Si-NP in the material, preventing aggregation phenomena; on the other hand, it improves silica affinity with the polymer matrix, giving rise to chemical interactions between NPs and the polymer matrix.

A common strategy of Si-NPs surface functionalization is based on physical interactions: interactions such as hydrogen bonding or electrostatic interactions have been exploited to anchor surfactants [49] or macromolecules [50] on Si-NPs, even though the weakness of the bond involved, make the surface coating easily detachable from the NPs. For this reason, chemical surface modification involving covalent bonds is more effective. In this context, organofunctional silane coupling agents, whose general structure is R-$(CH_2)_n$-SiX_3 (where X represents the hydrolysable groups, typically chloro, methoxy or ethoxy groups and R is the non-hydrolysable organofunctional group) are the most efficient modifier agents [51]. The R group is fundamental to introduce new functionalities on Si-NPs surface; some relevant examples are reported in Table 1The chemical modification of Si-NPs occurs via the hydrolysis of silane X groups and their subsequent condensation with silanol groups present on the surface of Si-NPs surface, forming new siloxane bonds (Scheme 1).

.

The chemical modification of Si-NPs occurs via the hydrolysis of silane X groups and their subsequent condensation with silanol groups present on the surface of Si-NPs surface, forming new siloxane bonds (Scheme 1).

Table 1. Typical coupling agents used for silica surface modification.

Name (abbreviation)	Chemical structure	Refs
3-aminopropyltriethoxysilane (APTES)	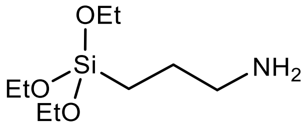	[52–55]
3-mercaptopropyltriethoxysilane (MPTES)	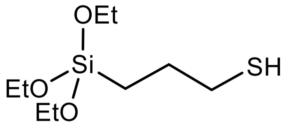	[56–59]
Vinyltriethoxysilane (VTS)	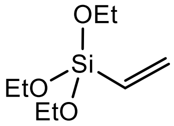	[60–63]
Methacryloxypropyltrimethoxysilane (MPTMS)	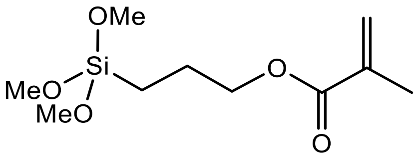	[64–67]

3-glycidyloxypropyltrimethoxysilane (GPTMS)	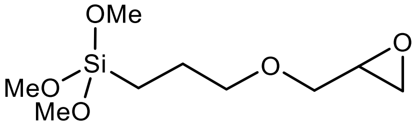	[68–71]
Methyltrichlorosilane (MTS)	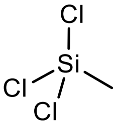	[72–75]

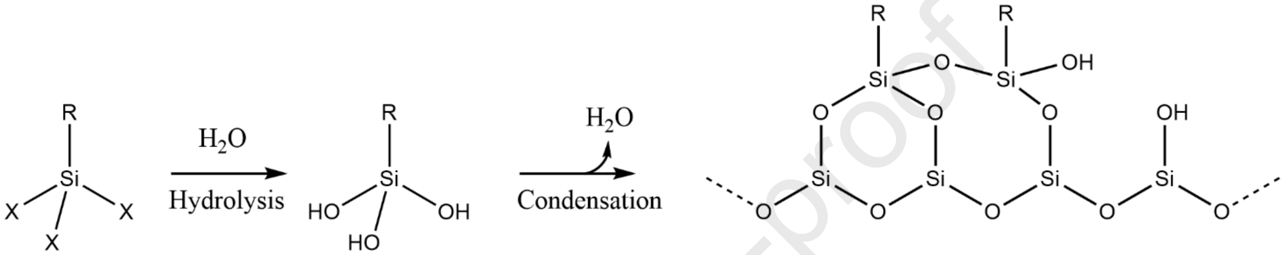

Scheme 1. Hydrolysis of an organosilane molecule and the following condensation with surface silanol groups.

Si-NPs functionalization is generally conducted with a post-synthetic grafting method, where the NPs synthesis and the organosilane functionalization are executed in consecutive steps. This process does not alter the size and size distribution of NPs and is usually carried out in nonaqueous systems to guarantee the direct grafting of organosilane on the silica surface. On the other hand, despite aqueous solvent causes uncontrollable hydrolysis and condensation reactions, it is a more favourable method for large-scale production [76]. As an alternative, the one-pot synthesis method requires the combination of a tetraalkoxysilane and a trialkoxysilane for the direct synthesis of functionalized Si-NPs [77]. This co-condensation strategy reduces both the time and the energy required by the post-modification approach and, above all, prevents the self-condensation of the alkoxysilane modifiers because these molecules are completely incorporated in the silica structure, both on the surface and in the core. Therefore, the one-pot approach guarantees a more homogeneous and quantitative incorporation of organosilane, preventing the aggregation phenomena of the NPs [78,79].

3. Macromolecules functionalized Si-NPs: the Hairy NPs

The functionalization of Si-NPs with small organic molecules allows their dispersion within organic matrices and introduces additional functionalities to favor the chemical interaction between Si-NPs and matrices. However, in recent years bonding end-tethered polymer chains to NPs surface has been considered with increasing attention because of the possibility to originate a wide range of new hybrid materials with broad applications in fields including sensors, information storage devices, medical diagnostic and catalysis, depending on the combination of NPs and the polymer brush. These hybrid particles, called Hairy NPs (HNPs), defined by Fernandes *et al.* [80] provide higher affinity between the inorganic particle and the organic component in polymer NC compared with NPs functionalized with smaller molecules, drastically improving the interfacial interactions between the NC phases.

Depending on the polymer chain length and chemical composition, it is possible to distinguish different types of HNPs (Figure 4). In the homopolymer condition, where the polymer chemistry is the same, monomodal, bimodal or disperse brushes can be obtained. Specifically, the first are NPs grafted with polymer chains of the same molecular weight, the second ones involve densely grafted short brush and sparsely grafted long brush and the last ones consist of polymer chains of various lengths. On the other side, mixed brushes HNPs are obtained when two polymers with different chemical composition are grafted on NPs.

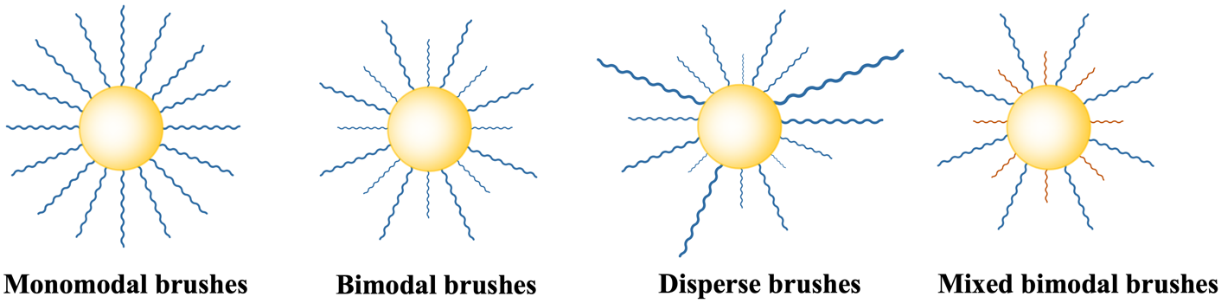

Figure 4. Schematic representation of HNPs with monomodal, bimodal, disperse and mixed bimodal brushes (from left to right).

The earliest examples of functionalization of inorganic particles with organic macromolecules date back to the 1950s, when polymers were used as stabilizing agents for colloidal dispersions. Originally, polymers were used as steric stabilizers by exploiting physisorption. The idea of grafting polymers onto particles by forming chemical bonds was only developed in the 1980s [81].

3.1 Synthesis of Si-HNPs

The three main approaches reported for the HNPs synthesis are: i) the one-pot or templated method, ii) the grafting-to and iii) grafting-from approaches (Figure 5).

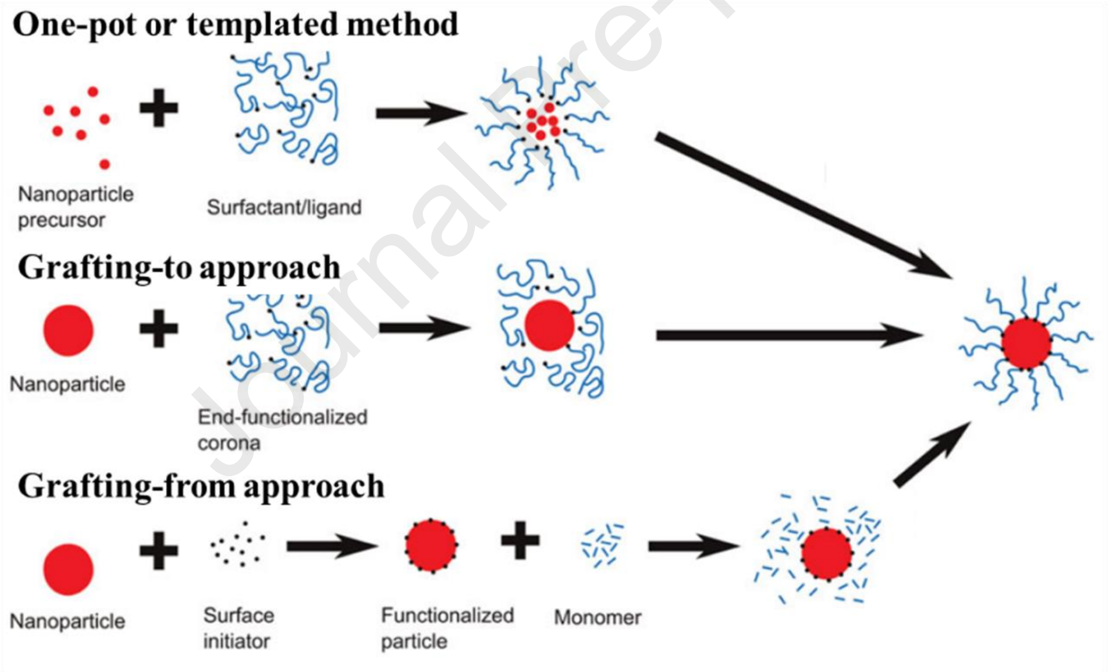

Figure 5. Synthetic strategies for the synthesis of HNPs. Reprinted with permission from [80].

The one-pot method, also defined as "grafting-through", involves the anchoring of polymers with the simultaneous synthesis of the NPs core, generally with the Stöber synthesis. Even if this method allows to achieve high NPs dispersion, preventing the aggregation issues, however, this approach can only be applied to polymers that are soluble in the same solvent where Si-NPs synthesis takes place, i.e. hydrophilic brushes such as polyethylene glycol (PEG). In this context, Zhang *et al.* [82] exploited a silane-terminated PEG chain that self-organizes in the aqueous reaction mixture in the presence of CTAB so that, after the formation of silica core, modified PEG chains remain anchored forming the polymer shell. A similar procedure is described by Akbari *et al.* [83], who used TEOS, ammonia and silane-terminated PEG, in the absence of surfactants.

The "grafting-to" approach involves the anchoring of a pre-formed polymer onto the surface of silica. By using adequately end-functionalized polymers, it is possible to directly anchor a polymer chain onto the NPs surface. As an example, Si-NPs can be grafted with polymers by exploiting the reaction of surface silanols with succinic anhydride-modified chains, as reported by Tai *et al.* [84] Alternatively, organosilanes can be used to introduce reactive functional groups on Si-NPs surface, which can further react with polymer chains. In this context, the use of "click" chemistry, such as alkyne-azide [85,86], was applied by Wu *et al.* [87] to synthesize mixed-grafted Si-NPs, functionalized with both polystyrene (PS) and poly(4-vinylpyridine). As an alternative, Kotsuchibashi *et al.* [88] applied the metal-free thiol-ene "click" chemistry to anchor thiol-terminated poly(2-(diethylamino)ethyl methacrylate and poly(N-isopropylacrylamide) to vinyl-modified Si-NPs. In addition, a combination of "click" chemistry with RAFT/ATRP has also been reported in the literature [89–91]. As an alternative, the amino groups on the surface of SiO_2 NPs modified with APTES can react with succinic anhydride-functionalized polymers. For example, Yuan *et al.* [92] followed this route for the synthesis of SiO_2 HNPs with polypropylene shells, Wei *et al.* [93] for PS and Tripaldi *et al.* [94] for polybutadiene (PB, Scheme 2).

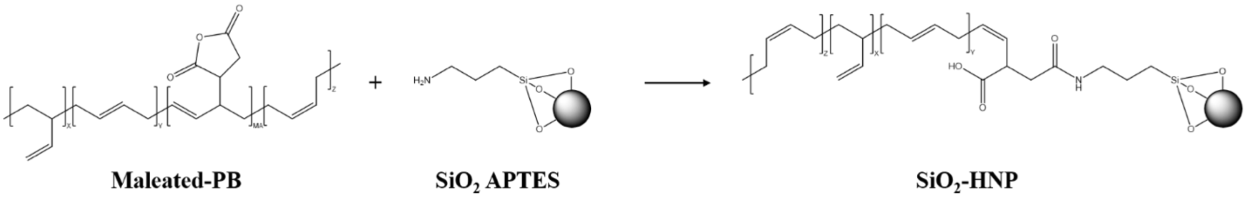

Scheme 2. Synthetic strategy for the synthesis of Si-HNPs with PB shell. Adapted from [94].

The "grafting-from" approach involves the growth of the polymer chains from a solution of the monomer, starting from chemical initiators anchored onto the surface of the particles. The polymer is synthesized through a class of chemical methods known as controlled radical polymerization (CRP), among which Atom Transfer Radical Polymerization (ATRP) and Reversible Addition-Fragmentation Chain Transfer (RAFT) polymerization are the most popular [95]. Thanks to the mechanism involved, CRP provide better control over molecular weight and dispersity of the polymer chains [95–97]. Overall, "grafting-from" synthesis of HNPs is preferred in those applications where very high grafting densities (i.e., number of chains per NPs surface area) are desirable, since these approaches can produce HNPs with up to 1.2 chains/nm^2 [98]. In addition, "grafting-from" allows the direct synthesis of block co-polymer shells with specific composition, and NPs with bimodal brushes, *i.e.* different polymers anchored onto the same NP core [99,100]. However, due to the much easier synthetic conditions, characterization and lack of contaminants of the polymer shell, "grafting-to" approaches are preferred when lower grafting densities are required.

3.2 Properties and characteristics of Si-HNPs

Among the properties of HNPs, the most significant one is the polymer grafting density, σ, previously defined as the number of polymer chains per unit of surface area (Eq. 6).

$$\sigma = \frac{chains}{nm^2} \qquad \textit{(Eq. 6)}$$

This parameter affects the conformation of grafted polymer chains along with NPs size, degree of polymerization of the polymer shell, as well as the solvent or matrix in which the HNPs are dispersed. The study of the polymer shell conformation is crucial because it affects both the behaviour and properties of HNPs, especially when embedded in polymers. Several studies have been dedicated to understand and model the conformation of polymer chains tethered to NP cores.

The first theoretical model of the conformation of polymer brushes, developed by De Gennes and Alexander in the 1970s [101,102], predicted that the conformation of a grafted polymer chain and hence the thickness h of the grafted polymer layer onto a flat surface depend on the parameters "σ" of the polymer. When the radius of gyration R_g of the grafted chains is smaller than the average distance between grafting points, the molecules are stretched, and their length is proportional to N, which is the degree of polymerization of the polymer chains [101]. This conformation is known as the concentrated polymer brush (CPB), or simply "brush" regime.

Conversely, when grafting points are placed at a sufficient distance from each other, polymer chains form random coils onto the grafted surface, creating the so-called dilute polymer brush (DPB) or "mushroom" regime. In this case, the thickness of the polymer layer scales like $N^{3/5}$.

Daoud and Cotton [103] extended this model to star polymers, consisting of a spherical polymer core with radius r_0 with f polymer chains of monomer length l grafted around it. By assuming that i) the degree of polymerization of the polymer chains, N, is uniform; ii) polymers are immersed in a good solvent and iii) the curvature effects (differently from polymers grafted onto a flat surface), the polymer conformation is also a function of the distance from the core. By dividing the polymer branches into spherical areas, Daoud and Cotton distinguished two different regions in the star polymer regime: the unswollen region, close to the star polymer core, where the polymer is more concentrated, and the swollen region, far from the core, where the polymer is more diluted.

Star polymers are similar to HNPs because they are both constituted by polymer chains grafted to a spherical core. Ohno *et al.* [104] and Dukes *et al.* [105] extended this theoretical framework to the case of HNPs, studying the effect of N and σ on the chain conformation. In particular, they introduced the reduced grafting density σ* (Eq. 7).

$$\sigma^* = \sigma \cdot l^2 \qquad (Eq.\ 7)$$

Based on these two parameters, their results are summarized in Table 2. Briefly, three possible regimes were identified for polymer chains grafted onto NPs: the "mushroom" regime (Figure 6a), the semi-dilute polymer brush or SDPB regime (Figure 6b) and the concentrated polymer brush or CPB regime ((Figure 6c), each of which shows a different dependence on grafting density and polymerization degree.

Since the HNPs surface is curved, the polymer chains are more densely packed close to the surface of the core. For this reason, Ohno *et al.* [104] determined the presence of a critical radius r_c that marks the transition between the CPB regime (closer to the core) and SDPB regime in HNPs (Eq. 8):

$$r_c = r_0 \sigma^{*1/2} \nu^{*\,-1} \qquad (Eq.\ 8)$$

where ν^* is a steric parameter, and r_0 is the radius of the HNP core.

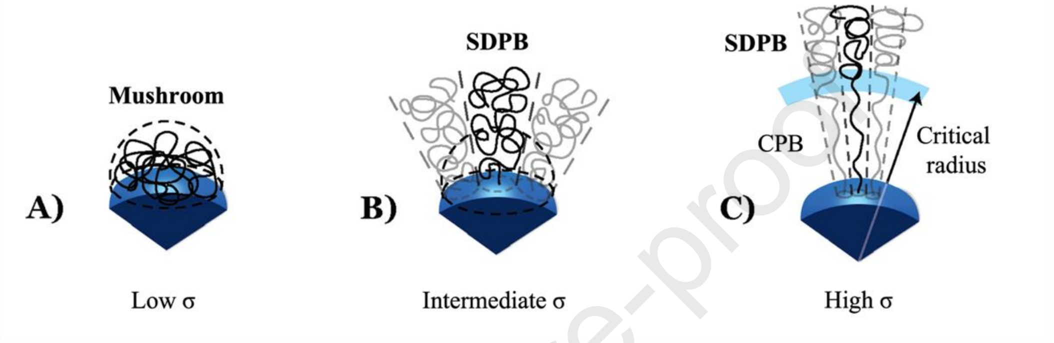

Figure 6. Schematic representation of a) mushroom regime, b) semi-dilute polymer brush and c) concentrated polymer brush for HNPs. Adapted from [105].

Table 2. Conformation of polymer brushes and scaling of the polymer shell thickness (h) as a function of polymerization degree N and reduced grafting density (σ*) for flat and spherical surfaces.

Curvature	Conformation	Scaling of h with N, σ^*
flat/spherical	Mushroom	$N^{3/5}$
flat	SDPB	$N^{1} \sigma^{*\,1/3}$
flat	CPB	$N^{1} \sigma^{*\,1/2}$
spherical	SDPB	$(N \sigma^{*\,1/3})^{3/5}$
spherical	CPB	$(N \sigma^{*\,1/2})^{x}$, $3/5 < x \leq 1$

Generally, sparsely grafted HNPs will exhibit “mushroom”-type conformation of polymer chains. Because of steric effects, HNPs synthesized by “grafting-to” will be generally in the mushroom regime, while HNPs synthesized by "grafting-from" will exhibit SDPB or CPB conformations. A good way to easily estimate the polymer shell regime of HNPs based on grafting density and radius of gyration R_g of the polymer shell was proposed by Brittain *et al* [106], introducing the *reduced tethered density* Σ, defined as follows (Eq. 9):

$$\Sigma = \sigma\, \pi\, R_g^2 \qquad (\mathit{Eq.}\ 9)$$

Then, based on the average results from several studies, they identified three possible regimes depending on the value of Σ: mushroom regime at $\Sigma < 1$, mushroom-to-brush transition regime at $1 < \Sigma < 5$, and brush regime at $\Sigma > 5$. It is important to point out that the R_g of the polymer depends on the solvent, and thus solvent effects can impact the polymer conformation in HNPs.

4. Si-NPs and Si-HNPs in NC materials

The introduction of Si-NPs into polymer matrices is a common strategy to produce materials with improved functional properties and specific technological applications [107,108] (Figure 7).

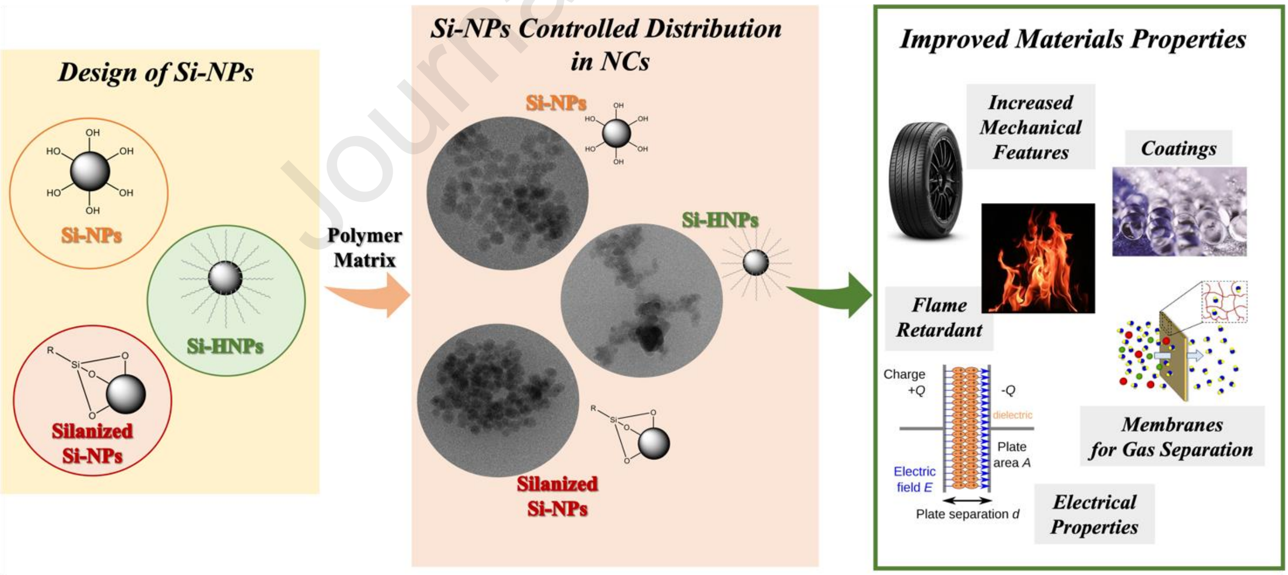

Figure 7. Preparation of polymer NCs with bare, silanized and polymer grafted Si-NPs for different technological applications. TEM micrographs are adapted from [94].

Briefly, the preparation of NCs containing Si-NPs includes: i) blending, i.e. the mixing of pre-synthetized Si-NPs into the polymer (which is deeply described in the present review); ii) sol−gel process, that involves the *in situ* synthesis of particles in the presence of a preformed organic polymer or simultaneously during the monomer polymerization; iii) *in situ* polymerization, that consists of the dispersion of pre-synthetized Si-NPs in the monomer(s) first, followed by the polymerization [9]. Different types of polymer matrices can be used, such as thermoplastics, thermosets and elastomers.

Firstly, the main advantage of polymer NCs over conventional composites is the presence of huge interfacial area between the inorganic nanofiller and the organic matrix, because of the nanoscale size of filler particles, providing a very high surface-to-volume ratio. This phenomenon is commonly referred to as the “nano-effect” and produces enhanced mechanical and physical properties.

Therefore, polymer NCs not only combine the properties of Si-NPs (e.g. rigidity and thermal stability) and organic polymers (e.g. flexibility, dielectric, ductility and processability). Moreover, the synergic interaction between the two components provides the material with new and improved physical-chemical, thermal and mechanical features. Actually, these new features originate from the interfacial interaction between filler, which provides an extremely high surface area, and polymer that is maximized in NCs. As consequence, it is mandatory: i) to improve the NPs-polymer interactions, ii) to balance of NPs-NPs and NPs-polymer interactions and iii) to control the NC morphology considering the dispersion and distribution of Si-NPs into the polymer matrix [109–111].

In fact, Si- NPs distribution and dispersion within the polymer matrix should be accurately tailored to obtain high-performance NCs. Excessive agglomeration, leading to phase separation, strongly reduces the effect of the filler in the NCs by limiting the interfacial area between the two components. In this context, it is crucial to keep in mind the distinction between filler dispersion and filler distribution, illustrated in Figure 8.

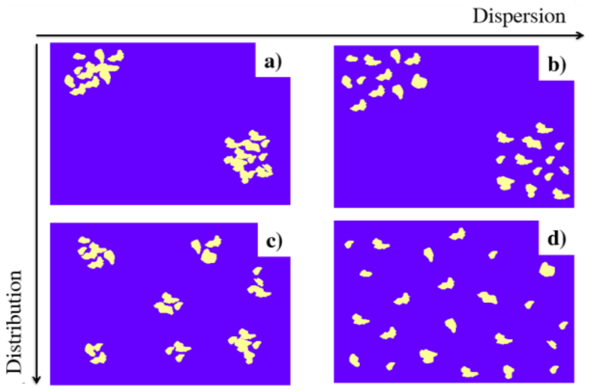

Figure 8. Schematic illustration of filler dispersion and distribution in polymer NCs: a) Poor dispersion, poor distribution; b) good dispersion, poor distribution; c) poor dispersion, good distribution and d) good dispersion, good distribution.

While good dispersion indicates that individual filler NPs are separated from each other instead of forming aggregates or clusters, distribution refers to the homogeneous presence of filler in the whole polymer matrix [112].

A trade-off between dispersion and distribution has to be achieved to tailor the properties of the NC materials. In fact, a good dispersion is always desirable to produce homogeneous properties in the final macroscopic material. On the other hand, the presence of NP-NP and NP-polymer interactions and their balance determines NPs spatial distribution and organization, which affect the macroscale properties of the hybrid materials. Recently, the improved properties of the NCs have been attributed to the ability of NPs to self-assemble into alternative structures like sheets, vesicles, percolating clusters and so on, which will be discussed more in-depth in the next section.

5. Si-NPs and Si-HNPs self-assembly in NCs materials

5.1 An overview of the self-assembling process

Self-assembly is the process by which disordered building blocks, such as atoms, molecules or NPs, spontaneously organise into a macroscopic structure with a higher level of structural complexity [113].

By self-assembling these building blocks, it is possible to obtain novel organizations, having new collective properties completely different from those of a single NP. In this way, a great variety of structures on multiple length scales can be formed, provided that a complete control of the morphologies and surface properties of the building block is achieved.

The first study which introduced the term self-assembly [114] dates back to 1983, when Nuzzo and Allara, described the formation of a closed-packed monolayer of gold surfaces grafted with alkyl disulfides as a “self-assembled monolayer”. However, already in 1935, Langmuir and Blodgett [115] evidenced the formation of a close-packed arrangement of amphiphilic molecules on liquid and solid surfaces, while in 1946 Bigelow [116] observed that long-chain alkylamines on the surface of platinum form a densely packed monolayer. Many examples of self-assembly processes are also present in nature [117], but only later they were recognized for what they were. Biological self-assembly exploits different lock-and-key, steric constraints hierarchical forces to drive specifically the species organization in viruses or globular proteins. It could be argued that the investigation of the self-assembly processes of non-living species could represent a way to understand more deeply also the living systems.

Self-assembly can be primarily classified in static and dynamic self-assembly processes. Static self-assembly, also called equilibrium self-assembly, usually requires an energetic input and leads to the minimization of the system free energy, thus reaching a thermodynamic local or global equilibrium. This is the case of lipid double layers formation and protein folding [118].

However, kinetic constraints can also be present, hindering the equilibrium state reaching or, on the contrary, obstructing the system’s return to the equilibrium state (non-equilibrium self-assembly) [119]. This is particularly relevant for polymer NCs preparation, where non-equilibrium structures can be achieved, due to the strong interparticle interactions, slow mobility and relaxation of the NPs in the polymer matrix [120].

Even if self-assembly is defined as a spontaneous process, the building blocks distribution can be directly controlled by an external influence (e.g. magnetic or electric fields, irradiation), obtaining a system which resides on an energetic minimum caused by a continuous influx of energy. This is the case of dynamic self-assembly. However, once the external input of energy stops, the minimum disappears, and the system disassembles. Examples of dynamic self-assemblies are also present in living cells where the interruption of the energy input leads to their death.

In addition to these two main kinds of self-assembly, templated self-assembly has also been identified when the interactions among the components lead to a specific organization with regular features in their environment [118]. This is the case of the crystal nucleation control by patterning the monolayers on which the crystallization occurs.

Some authors distinguish also the organization process derived by a selective functionalization of the building block as a directed self-assembly [121].

In recent years, many different synthetic and functionalization methods have been developed for the preparation of a variety of building blocks, engineering their structure and symmetry for a desired organization. NPs of different dimension, shape (rods, wires, rings, ellipsoids, cubes, triangular prisms), composition (core-shell) and surface chemistry have been prepared, thus setting the basis for different studies on their respective self-organization capabilities and resulting collective mechanical, electronic, optical, and magnetic properties.

In the NPs self-assembly process rationalization, a combination of attractive and repulsive driving forces must be considered depending on the NPs morphologies, interparticle interactions and external environment [122].

5.2 Si-NPs organizations in Polymer Matrices

Along with the previously illustrated assisted self-assemblies, polymers have been also identified as useful directing agents in the NPs self-assemblies. In this case, it is necessary to consider that kinetics has a critical role in expanding the possibility to obtain non-equilibrium structures, due to the relatively low mobility, slow relaxation and strong interparticle interactions of NPs in polymer matrices [120]. Furthermore, the NPs addition leads to an entropic penalty due to the stretching and compressing of polymer chains resulting in some cases in the microphase separation of NPs in the polymer matrices.

In this context, the focus is on the control of the NPs dispersion and relative organizations in the polymer matrix, which directly affect the properties of polymer NCs. In detail, the material performances are determined by two interfacial interactions: the NPs interparticle interactions and the NPs-polymers interactions, which differently affect the final macroscopic properties [123]. All these parameters are strictly related to the NPs dispersion state, which can be controlled through the energetic interactions or by entropic factors. However, the combination of van der Waals attraction forces, excluded volume interactions and depletion attraction forces experienced by the polymer matrix commonly leads to irreversible NPs aggregations. It is therefore necessary to act on these attractive forces by controlling the NP surface functionalization, morphology and the polymer NC preparation method, with subsequent treatments (annealing, sonication).

A general rule concerning the dispersion of NPs in polymer matrices was developed by Mackay *et al.* [7] who stated that the NPs segregate when the NP radius (R_{NP}) is bigger than the polymer radius of gyration (R_g), regardless of the polymer and filler chemistry. On the contrary, if R_{NP} is smaller than R_g the NPs disperse in the polymer matrix. This is because the increase in molecular contacts leads to an enthalpy gain, even if the process is entropically unfavourable.

In some applications, polymer NCs characterized by a connected network of particles (percolative network) are required. In this case, a partial aggregation of the particles is required and is better achievable at lower loadings with anisotropic NPs.

It is also necessary to consider that, depending on the employed NC preparation method (e.g., melt-mixing, solvent casting, extrusion, rapid precipitation, compression moulding and so on), the final NPs dispersion can be altered completely. In solvent-casted NCs, for example, the solvent and the evaporation rate play a fundamental role in governing NPs and polymer interactions.

In this context, Kumar and co-workers [124] investigated the changes in spherical Si-NPs organizations in a poly(2-vinyl pyridine) (P2VP) matrix by changing the solvent from methyl ethyl ketone (MEK) to pyridine (Figure 9a). By dispersing silica in MEK, a bound layer of the polymer on the silica surface forms and thus prevents particles agglomeration. However, at larger P2VP concentrations, NPs start to aggregate due to their bridging. On the contrary, when silica is dispersed in pyridine, a better solvent for the P2VP, a bound layer does not form and the NPs dispersion is governed by a balance between NPs electrostatic repulsions, polymer induced depletion attractions and kinetic slowdown of diffusion (depending on the polymer molecular weight).

More recently, similar studies were conducted by Lepcio and colleagues [125] on a system consisting of colloidal bare Si-NPs in a polymethylmethacrylate (PMMA) matrix. By combining TEM and ultra small-angle X-ray scattering (USAXS) analysis, three different NPs organizations were observed depending on the solvent involved during the polymer NC preparation (Figure 9b). The results show: i) individual particles dispersed in the matrix when acetone and ethyl acetate are applied for the polymer NC preparation; ii) Si-NPs aggregates with average sizes of approximately 400 and 500 nm using THF or toluene; iii) an intermediate distribution, consisting of three different populations of cluster sizes, with the 1:1 acetone-toluene mixture. By calculating the interaction enthalpies between Si-NPs and solvents, the authors were able to ascribe the Si-NPs organization to differences in terms of the amount of polymer adsorption and depletion attraction. In a subsequent study [126], the Authors found a significant influence of the NPs organization on relaxation and mechanical properties attributed to the presence of immobilized polymer segments in the vicinity of the NP surface and frustration of connected and intertangled chains. A unique reinforcing mechanism of chain bound clusters related to their internal structure was revealed.

Another description of Si-NPs behaviour in a polymer matrix is provided by Bouty *et al.* [127], who investigated the distribution of LUDOX Si-NPs in styrene-butadiene rubber (SBR) by solvent casting with dimethylacetamide. In this context, the NPs distribution inside the polymer matrix was studied by SAXS and TEM analysis, showing the aggregation of silica and the formation of clusters independently from the nature and the quantity of additives: octylytiethoxysilane (OCTEO) and bis(triethoxysilyl)propyltetrasulfide (TESPT). At increasing volume fractions of silica, a transition from individual clusters to a continuous network was observed (10 vol% of silica). In particular, at higher filler contents, the cluster size decreases from 170 to 115 nm, coherently with the formation of a filler network (Figure 9c). Authors concluded that NPs form individual clusters at low loading that can connect to form a continuous network at high silica loading and, under stretching, the NP acts as an additional cross-linked junction preventing the chain relaxations that are deformed at a larger amplitude than the pure polymer.

By large-scale molecular dynamics simulations Cheng *et al.* [128] demonstrated that also the evaporation process can dramatically affect the NPs assembly. Generally, NPs tend to accumulate near the film surface due to fast evaporation. However, in the case of immiscible NP/polymer systems, if fast evaporation is employed, a polymer layer forms on the surface and prevents the NPs diffusion.

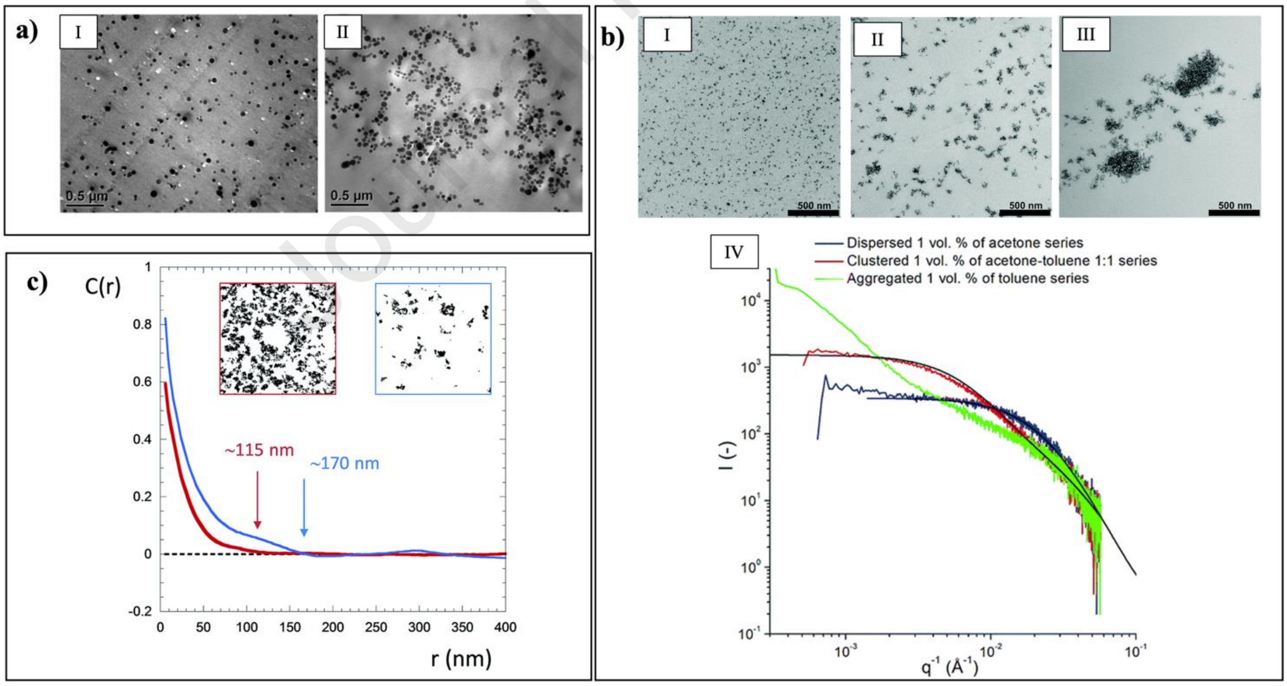

Figure 9. a) TEM images of 50 nm bare Si-NPs in a 14.7K P2VP matrix (10 wt%) prepared by solvent casting with MEK (I) and pyridine (II) [124]. b) TEM images of Si-NPs in PMMA matrix (1 vol%) prepared with acetone (I), 1:1 acetone-toluene mixture (II) and toluene (III). Dependence of intensity I vs the scattering vector length q obtained from USAXS data for teach solvent; the black lines

represent the trans for dispersed and clustered structures (IV) [125]. c) Radially averaged autocorrelation function C(r) vs the distance r for polymer NC including 10 vol% of Si-NPs with OCTEO (red) and 1 vol% Si-NPs with TESPT (blue); in both cases, the amount of additive is equal to 1 TEOS groups/nm^2 of SiO_2 [127]. Adapted from [124], [125] and [127].

The behavior of anisotropic Si-NPs in SBR NCs was investigated by Scotti *et al.* [33]. They studied the self-assembly of spherical and anisotropic Si-NPs with various aspect ratios, synthesized by a sol-gel method using TEOS and (3-mercaptopropyl) trimethoxysilane (MPTMS), in the presence of CTAB as a structure-directing agent. The influence of the particle morphology on the filler reinforcing effect was investigated, taking into consideration that the filler reinforcement effect in polymer NCs strongly depends on the rubber network, the hydrodynamic effect and the filler-rubber and filler-filler interactions. Scotti *et al.* demonstrated that, at increasing aspect ratio values, a stronger reinforcement of the rubber occurs. TEM analysis revealed that this improvement is associated with the self-organization of Si-NPs in ordered domains that guarantees a larger filler/polymer interface (Figure 10).

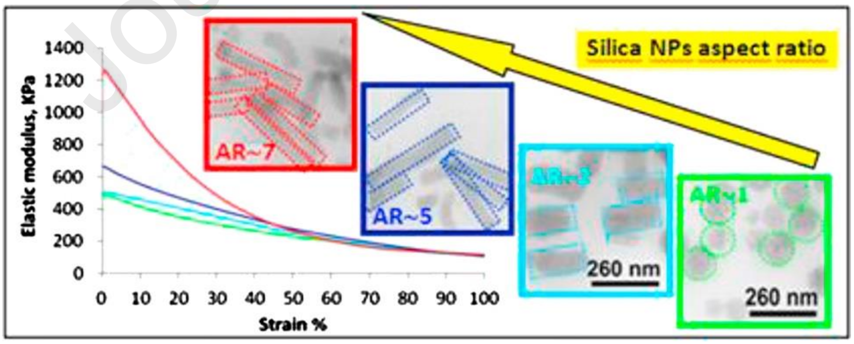

Figure 10. Silica rod-like particles with the highest aspect ratio provided stronger reinforcement of the rubber. Reprinted with permission from [33]

5.3 Si-HNPs organizations in Polymer Matrices

When Si-HNPs are embedded in a polymer matrix, their organization and spatial orientation are controlled by different factors. Considering a system in which HNPs are dispersed in a homopolymer matrix, it is clear that the NP core is not compatible with the polymeric matrix, whereas the interactions between the polymer brush and the matrix are enthalpically favoured.

However, HNPs self-assembly can be influenced by the conformational entropic penalty arising from the compression and extension of polymer brushes. As a result, HNPs in polymer matrices can arrange in a variety of superstructures by changing the polymer brush conformation.

As reported in Figure 11, by increasing graft polymer coverage (σ), it is possible to progressively go from spherical clusters to thick sheets, thin sheets, strings and finally well-dispersed particles. The same arrangements are independent on the type of polymer employed for the polymer NCs fabrication. Akcora and co-workers [129] performed experiments changing the polymer matrix molecular weight, evidencing an additional different trend.

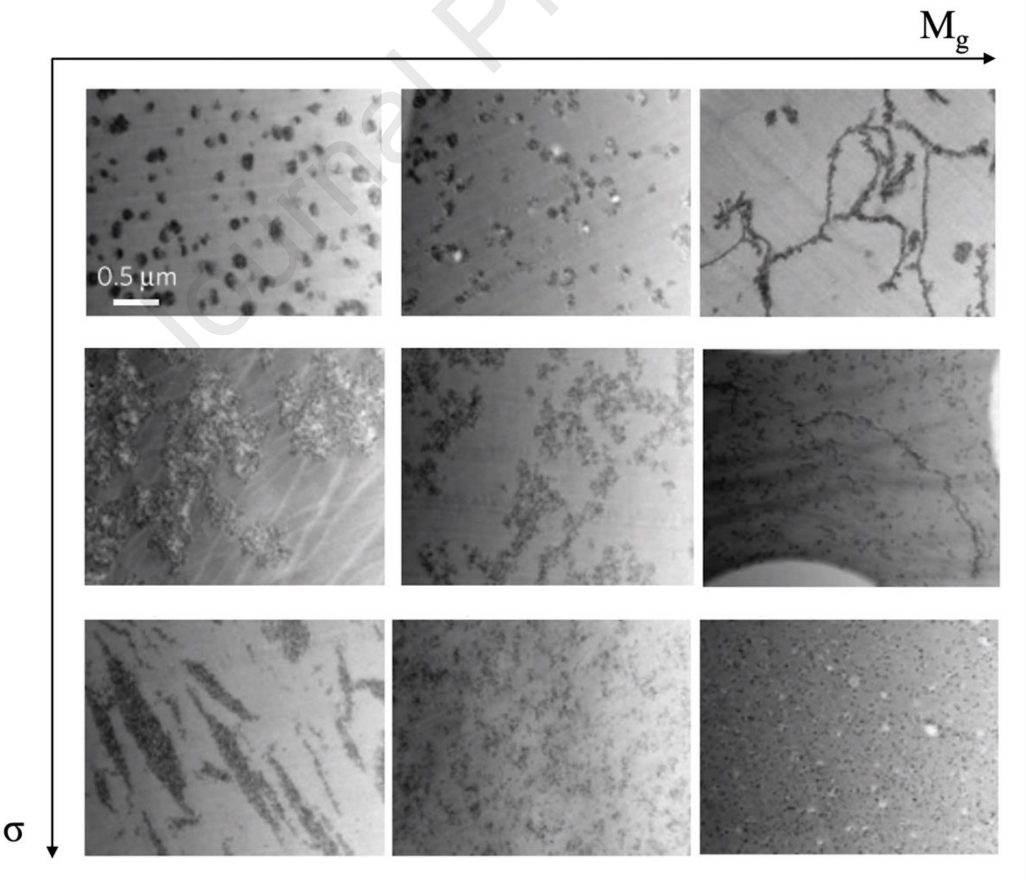

Figure 11. TEM micrographs of polymer NCs composed of PS-grafted Si-HNPs in a homopolymer matrix at different grafting densities (σ) and grafted polymer molecular weight (M_g). Adapted from [130].

Starting from this work, different studies [120,130,131] have focused on the investigation of the structural parameters influencing the assembled structures formed by HNPs in homopolymer matrices. To summarize all the available data regarding the HNPs assemblies, Kumar *et al.* [130] derived a graph (Figure 12) which allows to predict the NPs dispersion. The collected data regarded HNPs of similar size (diameter between 7 to 18 nm) at relatively low loadings (ca. 5 vol%) in a polymer matrix.

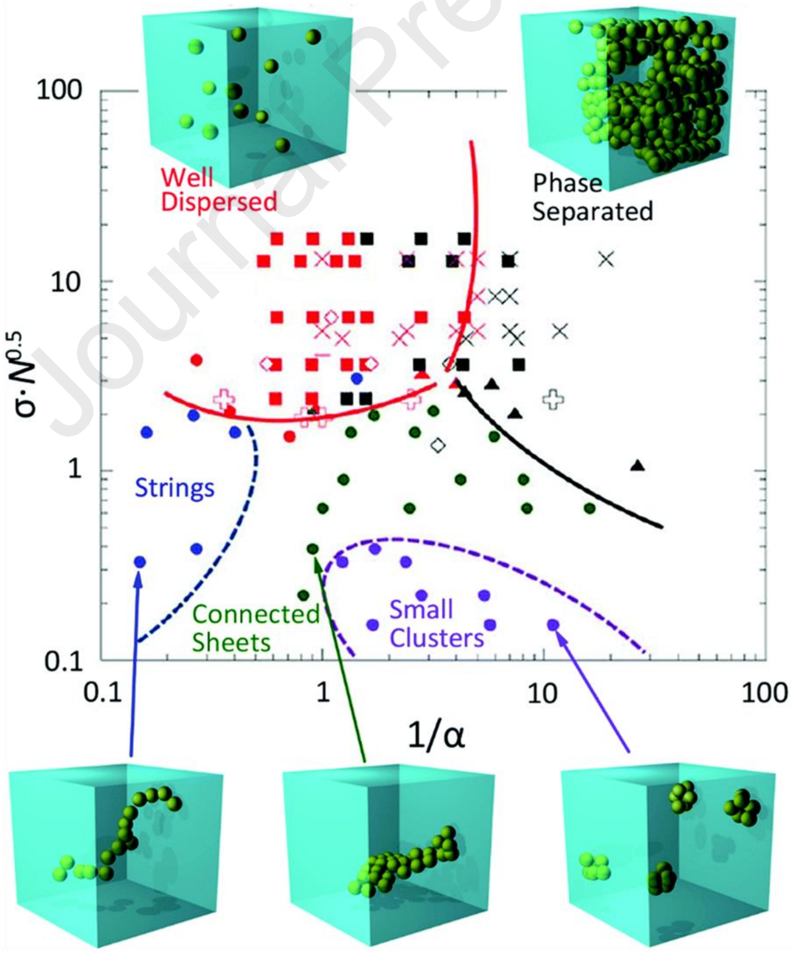

Figure 12. Morphology diagram based on all data available in literature. The graph plots σ·√N vs 1/α where, σ is the grafting density, α=P/N, N and P being the degree of polymerization of the grafted chains and matrix, respectively. Reprinted with permission from [120].

As reported in Figure 12, at high grafting densities ($\sigma \cdot\sqrt{N} > 2$), HNPs core-core attractions are negligible while grafted polymer chains stretch out forming a brush [131,132]. Therefore, the HNPs dispersion characteristics depend mainly on the polymer entropic effects: if the matrix chains have a lower molecular weight than the grafted brush ($\alpha > 0.2$), the free chains are able to penetrate and wet the brush, maximizing the translational entropy. Therefore, an attractive interaction between the two polymers arises and particles are completely dispersed. On the contrary, at increasing matrix molecular weight ($\alpha < 0.2$), the entropic penalty for the matrix to penetrate the grafted polymer brush increases and HNPs agglomeration and phase separation occurs. This phenomenon is also called *autophobic dewetting* [133] and consists of the depletion of the attraction between HNPs. This effect decreases with increasing surface curvature because smaller NPs suffer from less entropic penalty than larger ones or rod-like NPs [120,132,134,135].

At low grafting densities, the deformation of the polymer brush exposes the NPs surface. The consequent enthalpy increase drives the aggregation of the HNPs, which is instead limited by the steric repulsion between neighbouring polymer brushes. Thanks to the balance between extremely short-ranged interparticle attractions and the entropic penalty associated with the distortion of the polymer brush as NPs approach each other, HNPs organize in anisotropic structures inside the polymer matrix [130,136]. Hence, by varying the polymer brush features, it could be possible to control the interparticle attractions and the HNPs assembly, creating materials with tuneable properties. For example, Akora *et al.* [129] measured the linear and nonlinear rheology of NC based on 14-nm-diameter spherical silica particles grafted with PS chains embedded in PS matrix to delineate the practical usefulness of particle self-assembly. They demonstrated that the use of HNPs favours the creation of polymeric materials with significant reinforcement and at the same time without no stress drop-off at increasing strain (Figure 13): the gel-like structures that are formed owing to attractive core–core contacts at reduced polymer grafting on HNPs apparently do not give large stress overshoots.

All these studies [129,137,138] were performed by dispersing Si-NPs grafted with PS chains in PS matrices of different molecular weights. However, it has been demonstrated that the same arrangements are independent on the type of polymer employed for the polymer NCs fabrication; indeed, similar results have been observed by Akcora *et al.* [139] with PMMA composites and by Green *et al.* [140] with poly(dimethylsiloxane) (PDMS) grafted Si-HNPs dispersed in PDMS. In this study, rheology experiments showed that the composites display solid-like behaviour only when the particles are aggregated and the presence of percolating particle clusters in the agglomerated samples allows for stress propagation through the system. Authors conclude that mechanical reinforcement in polymer NCs is purely based on the NPs, surmising that mechanical reinforcement is caused by the bridging of particles by the grafted polymer layers on Si-NPs and not due to the formation of “glassy” polymer layers on the NPs.

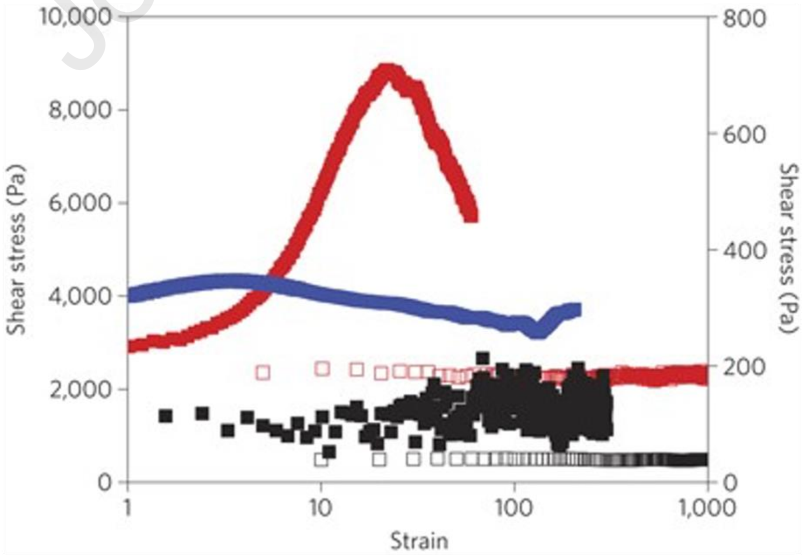

Figure 13. Shear stress *vs* strain of NC with matrix M=42 kg mol^{-1} (black) and 142 kg mol^{-1} (red) and of pure homopolymers. Each particle, on average, has 37 chains grafted to it, where each grafted

chain was of molecular mass of 106 kg mol^{-1}. The blue symbols are for a matrix with 142 kg mol^{-1} but for particles that have six chains grafted to them, with each of them of 158 kg mol^{-1}. The left axis is for the M=142 kg mol^{-1} and the right axis is for the 42 kg mol^{-1} matrix. The open symbols are for the homo-polymer and the filled symbols are for the NC. Reprinted with permission from [129].

More recent literature further confirms the reliability of this model for different homo-polymeric systems and the theory based on the work by Kumar *et al.* [130] In particular both Boonevide *et al.* [141] and Dhara *et al.* [142] observed self-assembly phenomena of polyisoprene (PI) grafted Si-HNPs when dispersed in PI matrix; in both cases, all polymeric components are synthesized with a RAFT polymerization. By varying σ and 1/α, for loading comprised between 5-15 wt%, TEM and SAXS analyses provide evidence of different structural organization, going from a well dispersed to sheets-forming conditions, in agreement with the plot provided by Kumar *et al.* [130] (Figure 14). Also in the case of PI-grafted silica [142], a specific HNP morphology was achieved at intermediate graft densities, consisting of a percolating particle network, with a significant reinforcement of the system, at a lower NP percolation loading threshold relative to other morphologies.

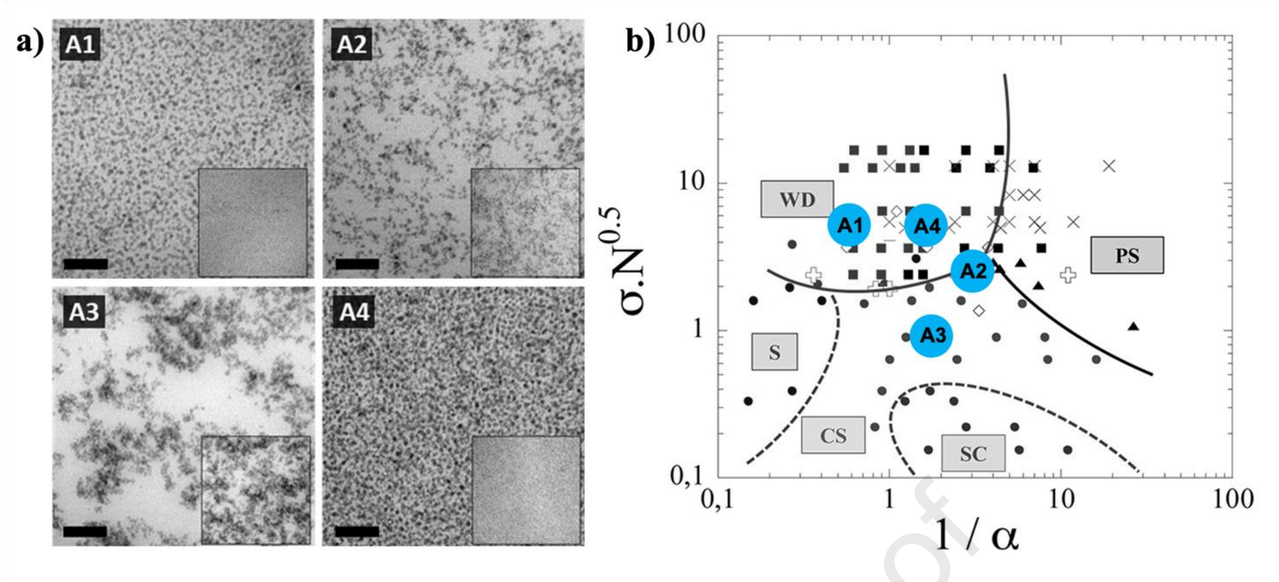

Figure 14. a) TEM images of PI grafted Si-HNPs in PI matrix, with N and σ equal to 104 kDa at 0.15 ch/nm^2 (A1), 20 kDa at 0.15 ch/nm^2(A2), 35 kDa at 0.035 ch/nm^2 (A3) and 38 kDa at 0.25 ch/nm^2 (A4). b) Representation in the morphology diagram of the various systems studied. Adapted with permission from [130] and [141].

Organization in anisotropic morphologies, specifically string-like structures and small clusters, was also observed by Bornani *et al.* [143] with polyethylene (PE) grafted Si-NPs, namely PE-g-SiO$_2$ NPs dispersed in a commercial high-density PE (HDPE), producing the so-called PE-g-SiO$_2$ NPs/PE NCs. In addition, this article highlights the role played by the dispersity of the matrix molecular weight and Si-NPs core size. These authors demonstrated that the usage of a commercial version of PI and PE and, hence, polymer matrices with a higher dispersity index, is associated to discrepancies in the filler organization, compared to the predictions based on the morphology plot (Figure 15). In addition, this study highlights how organized structures can serve as a tool to control nucleation and crystal growth in industrially relevant semicrystalline polymers.

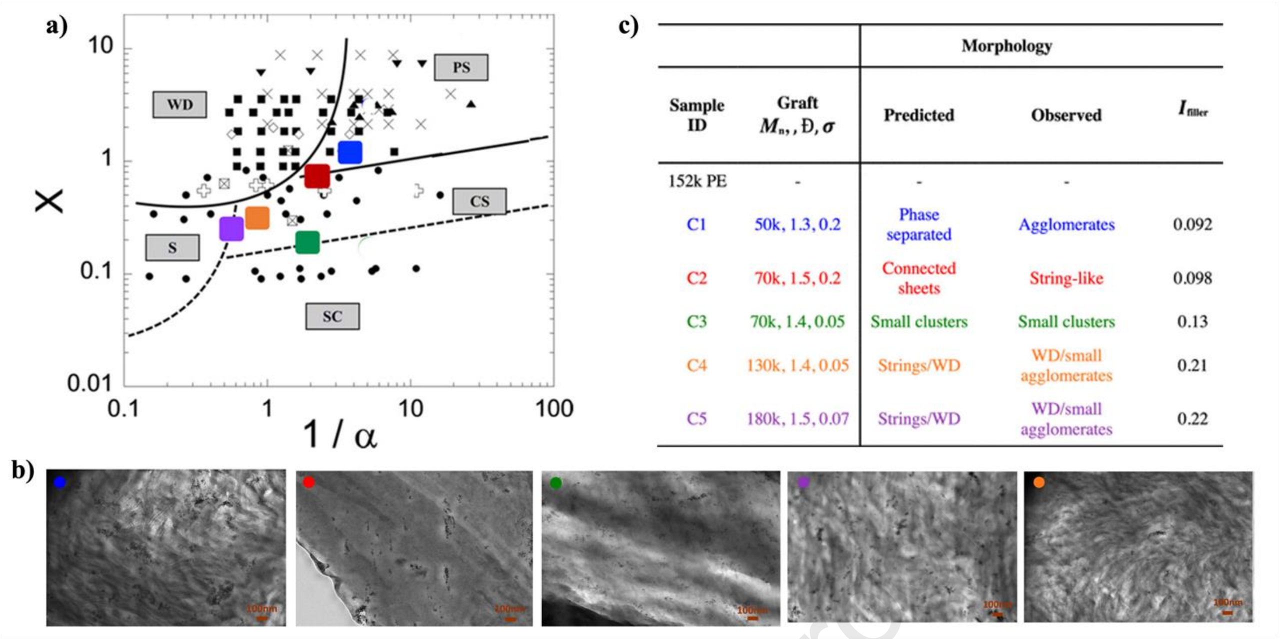

Sample ID	Graft M_n, Đ, σ	Morphology		
		Predicted	Observed	I_{filler}
152k PE	-	-	-	
C1	50k, 1.3, 0.2	Phase separated	Agglomerates	0.092
C2	70k, 1.5, 0.2	Connected sheets	String-like	0.098
C3	70k, 1.4, 0.05	Small clusters	Small clusters	0.13
C4	130k, 1.4, 0.05	Strings/WD	WD/small agglomerates	0.21
C5	180k, 1.5, 0.07	Strings/WD	WD/small agglomerates	0.22

Figure 15. a) Overcrowding parameter X of the predicted organizations of PE grafted Si-HNPs in a commercial 152 kDa PE matrix *vs* 1/α; b) TEM micrographs showing the organization of different graft MWs of PE-g-SiO_2 NPs in a commercial 152 kDa PE matrix; c) Summary of the grafting characteristics and the predicted and observed morphology of PE-g-SiO_2 NPs/PE NCs. Adapted with permission from [143].

The previously mentioned processes are temperature dependent as self-assembly is governed by a balance of entropic and enthalpic factors. Precisely, the temperature does influence not only the size of the aggregates but also their morphology [144]. On the contrary, the solvent employed doesn't play a crucial role in the particles arrangement, as long as it is favourable to the grafted chains [141]. However, in a system where the chemistry of the matrix and of the grafted chains are completely different, the enthalpic interactions become more dominant over the entropic ones and the Kumar diagram is not followed anymore [141]. A similar result has been found for thin films because the HNPs usually move to the air/film interface where they assemble in a variety of bidimensional superstructures, analogous to the bulk ones [130].

It must be noted that the formation of anisotropic arrangements is hindered for both homopolymer dispersed and bimodal grafted silica HNPs. These types of Si-HNPs are reported to be well-dispersed in a broad range of polymer matrix lengths, due to the sensible reduction in the core-core attraction forces guaranteed by the short grafted chains and the improved wettability of long chains [99,131,145,146]. On the other side, a fine control over core-core interactions is offered by mixed polymer brushes, which consist of bimodal HNPs with two chemically different polymers. In this context, Zhao *et al.* [100] compared the self-assembly properties of monomodal PS Si-HNPs and mixed bimodal with sparse grafted PS long chain and highly grafted P2VP short chain, dispersed in PS matrices by solvent-casting. Despite the presence of two different polymer lengths, mixed bimodal HNPs maintain the self-assembly properties because the core-core interactions are not strongly shielded compared to homopolymer bimodal HNPs. Indeed, this type of functionalization provides self-assembly with new morphologies: clumps with strings and thick strings with vesicles. Due to the higher dispersibility of bimodal polymer grafted HNPs in polymer matrices, Zhao *et al.* observed that the well-dispersed region and the phase separation are similar to the monomodal HNPs, but the region where anisotropic structures are formed is reduced (Figure 16). Composites prepared with these bimodal brush-grafted NPs showed improved mechanical and thermal properties when compared to monomodal-grafted nanoparticles, due to the improved NPs dispersion.

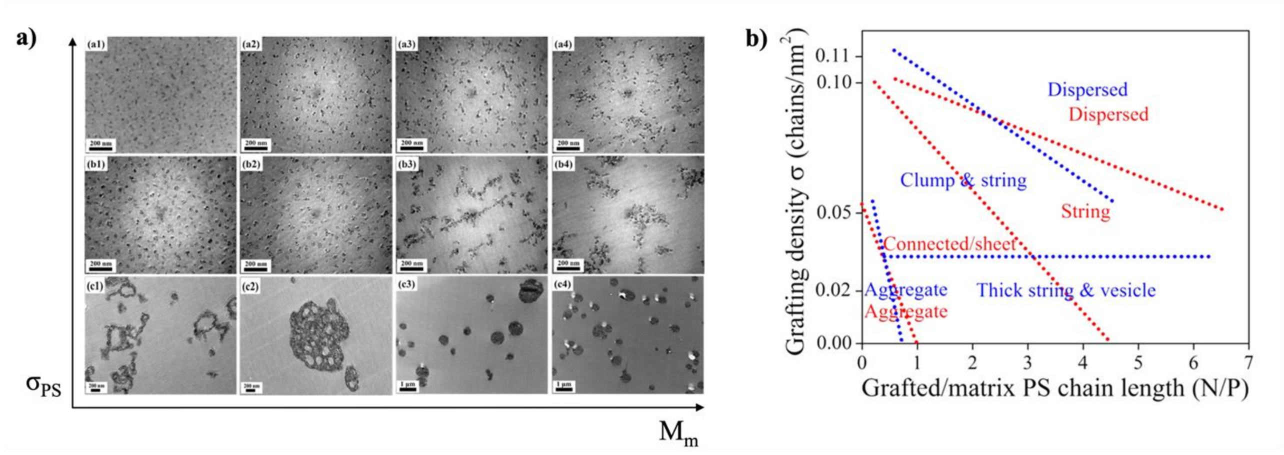

Figure 16. a) TEM micrographs of bimodal PS-P2VP grafted silica HNPs in PS matrices (5 wt%) at different PS grafting densities (σPS) and PS matrices molecular weight (Mm). b) comparison of the

dispersion state of bimodal PS-P2VP (blue) and monomodal PS (red) silica HNPs (core diameter: 14 ±4 nm) in PS matrices. Adapted with permission from [100].

Similar results were provided by Tang *et al.* [147] regarding mixed Si-HNPs (67 nm) grafted with PS (22.2 KDa, σ=0.31 ch/nm^2) and poly(tert-butylacrylate) (PtBA, 23.4 kDa, σ=0.54 ch/nm^2) dispersed in PtBA or poly(cyclohexyl methacrylate) (PCHMA) matrices with different molecular weights by solvent-casting technique. Indeed, in both matrices, they experimentally observed the formation of anisotropic structures such as worm-like domains, strings or small flocculates (Figure 17).

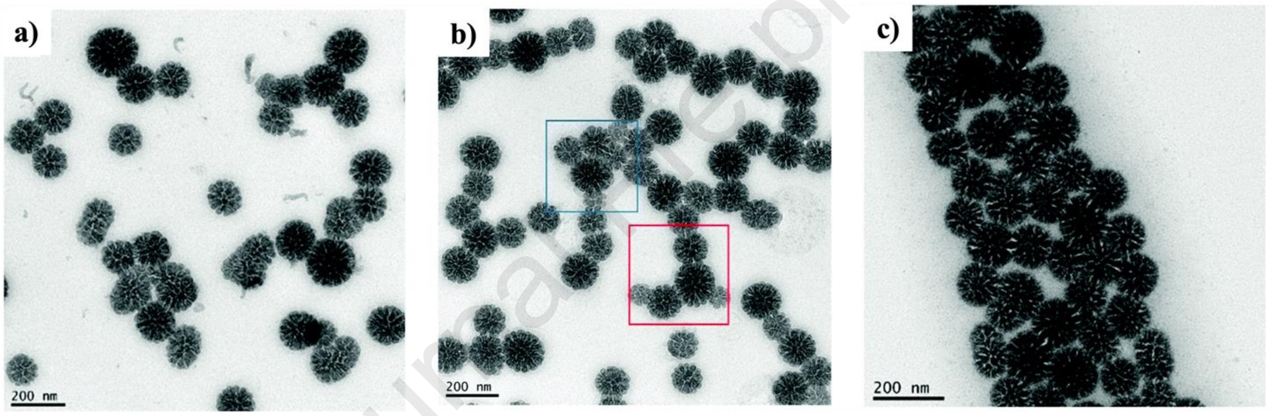

Figure 17. TEM images of mixed PtBA-PS grafted Si-NPs forming a) clusters in the 23 KDa PtBA matrix, b) strings in the 65 kDa PtBA matrix and c) worm-like structures in the 70 kDa PCHMA matrix. All the polymer NCs contain 1.5 wt% of silica HNPs. Reprinted with permission from [147].

6. Conclusion and Perspective

This review describes the use of Si-NPs and Si-HNPs in polymer matrices to significantly improve the properties of the final NC materials, which can be related to the self-organization behaviour of NPs. This self-assembly behaviour arises from a balance of attractive and repulsive interactions and may be controlled by tuning the surface chemistry of the NPs.

Firstly, the main preparation methods of spherical and anisotropic Si-NPs have been reported and discussed in connection with the chemical and morphological properties of particles, which strongly affect the dispersion, distribution, and self-assembling processes. Successively, the review analyzed the Si-NPs functionalization reactions with both small molecules, such as silane coupling agents, and with macromolecules, producing the so-called Si-HNPs. The organization of both anisotropic Si-NPs and Si-HNPs in polymer NCs has been discussed by analyzing the recent studies reported by significant numbers of researchers. Many Authors report scientific evidence of the organizational capability of Si-NPs and especially Si-HNPs in different polymeric matrices and highlight the positive impact of self-organized particles on improved materials properties.

The reported outcomes support the suitability of the strategy based on Si-NPs self-assembly as an effective approach for developing advanced functional polymer NCs. However, the relationship between NPs spatial distribution and macroscopic properties remains not completely understood. Further work will be needed to solve this issue and lead to a quantum leap in the property improvements and to the wider application of these materials.

Acknowledgements

E.M. thanks CORIMAV ("Consortium for the Research of Advanced Materials between Pirelli and Milano Bicocca University) for its support within the PCAM European Doctoral Program.

B.D.C. gratefully acknowledge Dr. Laura Tripaldi for her contribution related to HNPs state of the art.

References

[1] B.A. Grzybowski, C.E. Wilmer, J. Kim, K.P. Browne, K.J.M. Bishop, Self-assembly: From crystals to cells, Soft Matter. 5 (2009) 1110–1128. https://doi.org/10.1039/b819321p.

[2] L.S. Schadler, Polymer-Based and Polymer-Filled Nanocomposites, in: Nanocomposite Sci. Technol., 2003: pp. 77–153.

[3] G. Kickelbick, Introduction to Hybrid Materials, in: Hybrid Mater. Synth. Charact. Appl.,

2007: pp. 1–48.

[4] M. Grzelczak, J. Vermant, E.M. Furst, L.M. Liz-marza, L.M. Liz-Marzán, Directed self-assembly of nanoparticles, ACS Nano. 4 (2010) 3591–3605. https://doi.org/10.1021/nn100869j.

[5] S.N. Bhattacharya, M.R. Kamal, R.K. Gupta, Polymeric nanocomposites: theory and practice, 2008.

[6] R.A. Vaia, J.F. Maguire, Polymer nanocomposites with prescribed morphology: Going beyond nanoparticle-filled polymers, Chem. Mater. 19 (2007) 2736–2751. https://doi.org/10.1021/cm062693+.

[7] M.E. Mackay, A. Tuteja, P.M. Duxbury, C.J. Hawker, B. Van Horn, Z. Guan, G. Chen, R.S. Krishnan, General strategies for nanoparticle dispersion, Science (80-.). 311 (2006) 1740–1743. https://doi.org/10.1126/science.1122225.

[8] W.B. Russel, D.A. Seville, W.R. Schowalter, Colloidal Dispersions, 1989. https://doi.org/10.1017/CBO9780511608810.

[9] H. Zou, S. Wu, J. Shen, Polymer/Silica Nanocomposites: Preparation, characterization, propertles, and applications, Chem. Rev. 108 (2008) 3893–3957. https://doi.org/10.1021/cr068035q.

[10] J.S. Meth, S.G. Zane, C. Chi, D.J. Londono, B.A. Wood, P. Cotts, M. Keating, W. Guise, S. Weigand, Development of Filler Structure in Colloidal Silica–Polymer Nanocomposites, Macromolecules. 44 (2011) 8301–8313. https://doi.org/https://doi.org/10.1021/ma201714u.

[11] H.E. Bergna, Colloid Chemistry of Silica, Adv. Chem. 234 (1994) 1–47. https://doi.org/10.1021/ba-1994-0234.ch001.

[12] E.D.E.R. Hyde, A. Seyfaee, F. Neville, R. Moreno-Atanasio, Colloidal Silica Particle Synthesis and Future Industrial Manufacturing Pathways: A Review, Ind. Eng. Chem. Res. 55 (2016) 8891–8913. https://doi.org/10.1021/acs.iecr.6b01839.

[13] J.G. Croissant, K.S. Butler, J.I. Zink, C.J. Brinker, Synthetic amorphous silica nanoparticles:

toxicity, biomedical and environmental implications, Nat. Rev. Mater. 5 (2020) 886–909. https://doi.org/10.1038/s41578-020-0230-0.

[14] C. Drummond, R. McCann, S. V. Patwardhan, A Feasibility Study of the Biologically Inspired Green Manufacturing of Precipitated Silica, Chem. Eng. J. 244 (2014) 483–492. https://doi.org/10.1016/j.cej.2014.01.071.

[15] J. Schlomach, M. Kind, Investigations on the semi-batch precipitation of silica, J. Colloid Interface Sci. 277 (2004) 316–326. https://doi.org/10.1016/j.jcis.2004.04.051.

[16] W. Stöber, A. Fink, E. Bohn, Controlled Growth of Monodisperse Silica Spheres in the Micron Size Range, J. Colloid Interface Sci. 26 (1968) 62–69. https://doi.org/10.1016/0021-9797(68)90272-5.

[17] L.L. Hench, J.K. West, The Sol-Gel Process, Chem. Rev. 90 (1990) 33–72. https://doi.org/10.1021/cr00099a003.

[18] I.A. Rahman, V. Padavettan, Synthesis of Silica Nanoparticles by Sol-Gel: Size-Dependent Properties, Surface Modification, and Applications in Silica-Polymer Nanocomposites-A Review, J. Nanomater. 2012 (2012). https://doi.org/10.1155/2012/132424.

[19] S.-S. Choi, S.G. Lee, S.S. Im, S.H. Kim, Y.L. Joo, Silica Nanofibers from Electrospinning/Sol-Gel Process, J. Mater. Sci. Lett. 22 (2003) 891–893. https://doi.org/10.1023/A:1024475022937.

[20] G.H. An, S.Y. Jeong, T.Y. Seong, H.J. Ahn, One-pot fabrication of hollow SiO2 nanowires via an electrospinning technique, Mater. Lett. 65 (2011) 2377–2380. https://doi.org/10.1016/j.matlet.2011.05.043.

[21] L.P. Singh, S.K. Bhattacharyya, R. Kumar, G. Mishra, U. Sharma, G. Singh, S. Ahalawat, Sol-Gel processing of silica nanoparticles and their applications, Adv. Colloid Interface Sci. 214 (2014) 17–37. https://doi.org/10.1016/j.cis.2014.10.007.

[22] C.S. Choi, J.H. Yoon, Synthesis of Silica Nanowires by PECVD at Low Temperature Using Zn as a Catalyst, Appl. Phys. A Mater. Sci. Process. 108 (2012) 509–513.

https://doi.org/10.1007/s00339-012-7055-7.

[23] H. Zhang, C. Wang, E.C. Buck, L. Wang, Synthesis, Characterization and Manipulation of Helical SiO2 Nanosprings, Nano Lett. 3 (2003) 577–580. https://doi.org/10.1021/nl0341180.

[24] S.O. Obare, N.R. Jana, C.J. Murphy, Preparation of Polystyrene- and Silica-Coated Gold Nanorods and Their Use as Templates for the Synthesis of Hollow Nanotubes, Nano Lett. 1 (2001) 601–603. https://doi.org/10.1021/nl0156134.

[25] M. Fuji, T. Shin, H. Watanabe, T. Takei, Shape-Controlled Hollow Silica Nanoparticles Synthesized by an Inorganic Particle Template Method, Adv. Powder Technol. 23 (2012) 562–565. https://doi.org/10.1016/j.apt.2011.06.002.

[26] F. Dekker, R. Tuinier, A.P. Philipse, Synthesis of hollow silica nanocubes with tuneable size and shape, suitable for light scattering studies, Colloids and Interfaces. 2 (2018). https://doi.org/10.3390/colloids2040044.

[27] C. Gao, Z. Lu, Y. Yin, Gram-scale Synthesis of Silica Nanotubes with Controlled Aspect Ratios by Templating of Nickel-Hydrazine Complex Nanorods, Langmuir. 27 (2011) 12201–12208. https://doi.org/10.1021/la203196a.

[28] K.G. Lee, R. Wi, M. Imran, T.J. Park, J. Lee, S.Y. Lee, D.H. Kim, Functionalization Effects of Single-Walled Carbon Nanotubes as Templates for the Synthesis of Silica Nanorods and Study of Growing Mechanism of Silica, ACS Nano. 4 (2010) 3933–3942. https://doi.org/10.1021/nn100807r.

[29] M. Zhang, Y. Bando, K. Wada, Silicon Dioxide Nanotubes Prepared by Anodic Alumina as Templates, J. Mater. Res. 15 (2000) 387–392. https://doi.org/10.1557/JMR.2000.0061.

[30] A. Kuijk, A. Van Blaaderen, A. Imhof, Synthesis of Monodisperse, Rodlike Silica Colloids with Tunable Aspect Ratio, J. Am. Chem. Soc. 133 (2011) 2346–2349. https://doi.org/10.1021/ja109524h.

[31] C. Chen, L. Xie, Y. Wang, Recent Advances in the Synthesis and Applications of Anisotropic Carbon and Silica-Based Nanoparticles, Nano Res. 12 (2019) 1267–1278.

https://doi.org/10.1007/s12274-019-2324-9.

[32] X. Du, J. He, Elaborate Control over the Morphology and Structure of Mercapto-Functionalized Mesoporous Silicas as Multipurpose Carriers, Dalt. Trans. 39 (2010) 9063–9072. https://doi.org/10.1039/c0dt00194e.

[33] R. Scotti, L. Conzatti, M. D’Arienzo, B. Di Credico, L. Giannini, T. Hanel, P. Stagnaro, A. Susanna, L. Tadiello, F. Morazzoni, Shape Controlled Spherical (0D) and Rod-Like (1D) Silica Nanoparticles in Silica/Styrene Butadiene Rubber Nanocomposites: Role of the Particle Morphology on the Filler Reinforcing Effect, Polymer. 55 (2014) 1497–1506. https://doi.org/10.1016/j.polymer.2014.01.025.

[34] M.A.A. Abdelhamid, S.P. Pack, Biomimetic and Bioinspired Silicifications: Recent Advances for Biomaterial Design and Applications, Acta Biomater. 120 (2021) 38–56. https://doi.org/10.1016/j.actbio.2020.05.017.

[35] S. V. Patwardhan, Biomimetic and Bioinspired Silica: Recent Developments and Applications, Chem. Commun. 47 (2011) 7567–7582. https://doi.org/10.1039/c0cc05648k.

[36] R.H. Jin, J.J. Yuan, Synthesis of poly(ethyleneimine)s-silica hybrid particles with complex shapes and hierarchical structures, Chem. Commun. 1 (2005) 1399–1401. https://doi.org/10.1039/b417351a.

[37] P.C. Carman, Constitution of Colloidal Silica, Trans. Faraday Soc. 36 (1940) 964–973. https://doi.org/10.1039/tf9403600964.

[38] A. Rimola, D. Costa, M. Sodupe, J.F. Lambert, P. Ugliengo, Silica surface features and their role in the adsorption of biomolecules: Computational modeling and experiments, Chem. Rev. 113 (2013) 4216–4313. https://doi.org/10.1021/cr3003054.

[39] T. Jesionowski, Synthesis of organic–inorganic hybrids via adsorption of dye on an aminosilane-functionalised silica surface, Dye. Pigment. 55 (2002) 133–141. https://doi.org/10.1016/S0143-7208(02)00105-5.

[40] H.E. Bergna, W.O. Roberts, Colloidal Silica: Fundamentals and Applications, CRC Press,

2005.

[41] E.F. Vansant, P. Van Der Voort, K.C. Vrancken, Characterization and Chemical Modification of the Silica Surface, Amsterdam, 1995.

[42] A. Burneau, O. Barres, J. Gallas, J.C. Lavalley, Comparative Study of the Surface Hydroxyl Groups of Fumed and Precipitated Silicas. 2. Characterization by Infrared Spectroscopy of the Interactions with Water, Langmuir. 6 (1990) 1364–1372. https://doi.org/10.1021/la00098a008.

[43] S. Ek, A. Root, M. Peussa, L. Niinistö, Determination of the hydroxyl group content in silica by thermogravimetry and a comparison with 1H MAS NMR results, Thermochim. Acta. 379 (2001) 201–212. https://doi.org/10.1016/S0040-6031(01)00618-9.

[44] T.I. Suratwala, M.L. Hanna, E.L. Miller, P.K. Whitman, I.M. Thomas, P.R. Ehrmann, R.S. Maxwell, A.K. Burnham, Surface chemistry and trimethylsilyl functionalization of Stöber silica sols, J. Non. Cryst. Solids. 316 (2003) 349–363. https://doi.org/10.1016/S0022-3093(02)01629-0.

[45] D.W. Schaefer, T. Rieker, M. Agamalian, J.S. Lin, D. Fischer, S. Sukumaran, C. Chen, C.H. Beaucage, J. Ivie, C. Chen, G. Beaucage, C. Herd, J. Ivie, Multilevel Structure of Reinforcing Silica and Carbon, J. Appl. Crystallogr. 33 (2000) 587–591. https://doi.org/10.1107/S0021889800001199.

[46] D.R. Boverhof, C.M. Bramante, J.H. Butala, S.F. Clancy, W.M. Lafranconi, J. West, S.C. Gordon, Comparative Assessment of Nanomaterial Definitions and Safety Evaluation Considerations, Regul. Toxicol. Pharmacol. 73 (2015) 137–150. https://doi.org/10.1016/j.yrtph.2015.06.001.

[47] C.A. Gray, H. Muranko, Studies of Robustness of Industrial Aciniform Aggregates and Agglomerates - Carbon Black and Amorphous Silicas: A Review Amplified by New Data, J. Occup. Environ. Med. 48 (2006) 1279–1290. https://doi.org/10.1097/01.jom.0000251477.40643.2a.

[48] M.Z. Rong, M.Q. Zhang, W.H. Ruan, Surface Modification of Nanoscale Fillers for Improving Properties of Polymer Nanocomposites: A Review, Mater. Sci. Technol. 22 (2006) 787–796. https://doi.org/10.1179/174328406X101247.

[49] T.M. Wu, M.S. Chu, Preparation and Characterization of Thermoplastic Vulcanizate/Silica Nanocomposites, J. Appl. Polym. Sci. 98 (2005) 2058–2063. https://doi.org/10.1002/app.22406.

[50] X. Yang, T. Dai, Y. Lu, Synthesis of Novel Sunflower-Like Silica/Polypyrrole Nanocomposites via Self-Assembly Polymerization, Polymer (Guildf). 47 (2006) 441–447. https://doi.org/10.1016/j.polymer.2005.11.037.

[51] B. Arkles, Silane Coupling Agents: Connecting Across Boundaries, 3rd ed., Gelest Inc., 2014.

[52] E.J. Cueto-Díaz, A. Castro-Muñiz, F. Suárez-García, S. Gálvez-Martínez, M.C. Torquemada-Vico, M.P. Valles-González, E. Mateo-Martí, Aptes-based silica nanoparticles as a potential modifier for the selective sequestration of co2 gas molecules, Nanomaterials. 11 (2021). https://doi.org/10.3390/nano11112893.

[53] B. Ahn, D. Kim, K. Kim, I.J. Kim, H.J. Kim, C.H. Kang, J.Y. Lee, W. Kim, Effect of the functional group of silanes on the modification of silica surface and the physical properties of solution styrene-butadiene rubber/silica composites, Compos. Interfaces. 26 (2019) 585–596. https://doi.org/10.1080/09276440.2018.1514145.

[54] S.R. Karnati, D. Oldham, E.H. Fini, L. Zhang, Surface functionalization of silica nanoparticles to enhance aging resistance of asphalt binder, Constr. Build. Mater. 211 (2019) 1065–1072. https://doi.org/10.1016/j.conbuildmat.2019.03.257.

[55] K. Monjezi, M. Mohammadi, A.R. Khaz’ali, Stabilizing CO2 foams using APTES surface-modified nanosilica: Foamability, foaminess, foam stability, and transport in oil-wet fractured porous media, J. Mol. Liq. 311 (2020) 113043. https://doi.org/10.1016/j.molliq.2020.113043.

[56] I.I. Slowing, C.W. Wu, J.L. Vivero-Escoto, V.S.Y. Lin, Mesoporous silica nanoparticles for reducing hemolytic activity towards mammalian red blood cells, Small. 5 (2009) 57–62. https://doi.org/10.1002/smll.200800926.

[57] X. feng Kong, B. Yang, H. Xiong, Y. Zhou, S. guo Xue, B. qiang Xu, S. xing Wang, Selective removal of heavy metal ions from aqueous solutions with surface functionalized silica nanoparticles by different functional groups, J. Cent. South Univ. 21 (2014) 3575–3579. https://doi.org/10.1007/s11771-014-2338-0.

[58] A. Gottuso, F. Armetta, A. Cataldo, V.M. Nardo, F. Parrino, M.L. Saladino, Functionalization of mesoporous silica nanoparticles through one-pot co-condensation in w/o emulsion, Microporous Mesoporous Mater. 335 (2022) 111833. https://doi.org/10.1016/j.micromeso.2022.111833.

[59] F. Zhao, X. Yao, C. Liu, X. Ran, C. Wang, B. Lu, Mercapto-functionalized ordered mesoporous silica-modified PVDF membrane for efficiently scavenging Cd2+ from water, J. Environ. Manage. 302 (2022) 114103. https://doi.org/10.1016/j.jenvman.2021.114103.

[60] R. Ghamarpoor, M. Jamshidi, Synthesis of vinyl-based silica nanoparticles by sol–gel method and their influences on network microstructure and dynamic mechanical properties of nitrile rubber nanocomposites, Sci. Rep. 12 (2022) 1–15. https://doi.org/10.1038/s41598-022-19664-w.

[61] T. Meyer, S. Spange, S. Hesse, C. Jäger, C. Bellmann, Radical grafting polymerization of vinylformamide with functionalized silica particles, Macromol. Chem. Phys. 204 (2003) 725–732. https://doi.org/10.1002/macp.200390042.

[62] Z. Yang, H. Peng, W. Wang, T. Liu, Crystallization behavior of poly(ε-caprolactone)/layered double hydroxide nanocomposites, J. Appl. Polym. Sci. 116 (2010) 2658–2667. https://doi.org/10.1002/app.

[63] X. Jia, Y. Li, Q. Cheng, S. Zhang, B. Zhang, Preparation and properties of poly(vinyl alcohol)/silica nanocomposites derived from copolymerization of vinyl silica nanoparticles

and vinyl acetate, Eur. Polym. J. 43 (2007) 1123–1131. https://doi.org/10.1016/j.eurpolymj.2007.01.019.

[64] Q. Dong, Y. Ding, B. Wen, F. Wang, H. Dong, S. Zhang, T. Wang, M. Yang, Improvement of thermal stability of polypropylene using DOPO-immobilized silica nanoparticles, Colloid Polym. Sci. 290 (2012) 1371–1380. https://doi.org/10.1007/s00396-012-2631-0.

[65] W. Yang, L. Zhu, Y. Chen, One-step fabrication of 3-methacryloxypropyltrimethoxysilane modified silica and investigation of fluorinated polyacrylate/silica nanocomposite films, RSC Adv. 5 (2015) 58973–58979. https://doi.org/10.1039/c5ra10535h.

[66] J. Jiang, W. Wang, H. Shen, J. Wang, J. Cao, Characterization of silica particles modified with γ-methacryloxypropyltrimethoxysilane, Appl. Surf. Sci. 397 (2017) 104–111. https://doi.org/10.1016/j.apsusc.2016.11.075.

[67] I.D. Sideridou, M.M. Karabela, Effect of the amount of 3-methacyloxypropyltrimethoxysilane coupling agent on physical properties of dental resin nanocomposites, Dent. Mater. 25 (2009) 1315–1324. https://doi.org/10.1016/j.dental.2009.03.016.

[68] R. Suntako, Rubber Rail Pad Reinforced by Modified Silica Using GPTMS and Sulfenamide Accelerator, Polymers (Basel). 14 (2022). https://doi.org/10.3390/polym14091767.

[69] K. Fukuda, H. Yoshitake, Alternating copolymerization of functionalized silica nanoparticles, Polymer (Guildf). 165 (2019) 133–141. https://doi.org/10.1016/j.polymer.2019.01.036.

[70] C.H. Liu, C.Y. Pan, Grafting polystyrene onto silica nanoparticles via RAFT polymerization, Polymer (Guildf). 48 (2007) 3679–3685. https://doi.org/10.1016/j.polymer.2007.04.055.

[71] P. Vejayakumaran, I.A. Rahman, C.S. Sipaut, J. Ismail, C.K. Chee, Structural and thermal characterizations of silica nanoparticles grafted with pendant maleimide and epoxide groups, J. Colloid Interface Sci. 328 (2008) 81–91. https://doi.org/10.1016/j.jcis.2008.08.054.

[72] L. Dashairya, D.D. Barik, P. Saha, Methyltrichlorosilane functionalized silica nanoparticles-

treated superhydrophobic cotton for oil–water separation, J. Coatings Technol. Res. 16 (2019) 1021–1032. https://doi.org/10.1007/s11998-018-00177-z.

[73] H.S. Khoo, F.G. Tseng, Engineering the 3D architecture and hydrophobicity of methyltrichlorosilane nanostructures, Nanotechnology. 19 (2008). https://doi.org/10.1088/0957-4484/19/34/345603.

[74] S. Tao, Y. Wang, Y. An, Superwetting monolithic SiO2 with hierarchical structure for oil removal, J. Mater. Chem. 21 (2011) 11901–11907. https://doi.org/10.1039/c1jm12141c.

[75] N. Jumrus, J. Jompaeng, A. Panthawan, T. Kumpika, O. Wiranwetchayan, P. Sanmuangmoon, W. Sroila, E. Kantarak, P. Singjai, W. Thongsuwan, Transparency and water resistance of a superhydrophobic acrylic surface prepared using THF/IPA etching-assisted SiO2 NPs, Mater. Lett. 304 (2021) 130618. https://doi.org/10.1016/j.matlet.2021.130618.

[76] P. Van Der Van Der Voort, E.F. Vansant, Silylation of the Silica Surface A Review, J. Liq. Chromatogr. Relat. Technol. 19 (1996) 2723–2752. https://doi.org/10.1080/10826079608015107.

[77] H. Li, X. Chen, D. Shen, F. Wu, R. Pleixats, J. Pan, Functionalized Silica Nanoparticles: Classification, Synthetic Approaches and Recent Advances in Adsorption Applications, Nanoscale. 13 (2021) 15998–16016. https://doi.org/10.1039/d1nr04048k.

[78] E. Da’na, Adsorption of heavy metals on functionalized-mesoporous silica: A review, Microporous Mesoporous Mater. 247 (2017) 145–157. https://doi.org/10.1016/j.micromeso.2017.03.050.

[79] N. Tang, X. Liu, M.R. Jia, X.Y. Shi, J.W. Fu, D.X. Guan, L.Q. Ma, Amine- and thiol-bifunctionalized mesoporous silica material for immobilization of Pb and Cd: Characterization, efficiency, and mechanism, Chemosphere. (2021) 132771. https://doi.org/10.1016/j.chemosphere.2021.132771.

[80] N.J. Fernandes, H. Koerner, E.P. Giannelis, R.A. Vaia, Hairy nanoparticle assemblies as one-

component functional polymer nanocomposites: opportunities and challenges, MRS Commun. 3 (2013) 13–29. https://doi.org/10.1557/mrc.2013.9.

[81] D.H. Napper, Polymeric stabilization of colloidal dispersions, Academic Press, New York, 1984.

[82] Q. Zhang, Z. Ye, S.T. Wang, J. Yin, Facile one-pot synthesis of PEGylated monodisperse mesoporous silica nanoparticles with controllable particle sizes, Chinese Chem. Lett. 25 (2014) 257–260. https://doi.org/10.1016/j.cclet.2013.11.002.

[83] A. Akbari, R. Yegani, B. Pourabbas, Synthesis of poly(ethylene glycol) (PEG) grafted silica nanoparticles with a minimum adhesion of proteins via one-pot one-step method, Colloids Surfaces A Physicochem. Eng. Asp. 484 (2015) 206–215. https://doi.org/10.1016/j.colsurfa.2015.07.042.

[84] Y. Tai, J. Qian, Y. Zhang, J. Huang, Study of surface modification of nano-SiO2 with macromolecular coupling agent (LMPB-g-MAH), Chem. Eng. J. 141 (2008) 354–361. https://doi.org/10.1016/j.cej.2008.03.012.

[85] G. Bissadi, R. Weberskirch, Efficient synthesis of polyoxazoline-silica hybrid nanoparticles by using the “grafting-onto” approach, Polym. Chem. 7 (2016) 1271–1280. https://doi.org/10.1039/c5py01775k.

[86] S.S. Balamurugan, E. Soto-Cantu, R. Cueto, P.S. Russo, Preparation of organosoluble silica-polypeptide particles by “Click” chemistry, Macromolecules. 43 (2010) 62–70. https://doi.org/10.1021/ma901840n.

[87] L. Wu, U. Glebe, A. Böker, Synthesis of Polystyrene and Poly (4-vinylpyridine) Mixed Grafted Silica Nanoparticles via a Combination of ATRP and Cu I -Catalyzed Azide-Alkyne Click Chemistry, 1600475 (n.d.) 1–7. https://doi.org/10.1002/marc.201600475.

[88] Y. Kotsuchibashi, M. Ebara, T. Aoyagi, R. Narain, Fabrication of doubly responsive polymer functionalized silica nanoparticles via a simple thiol – ene click chemistry †, Polym. Chem. 3 (2012) 2545–2550. https://doi.org/10.1039/c2py20333b.

[89] J. Chen, M. Liu, C. Chen, H. Gong, C. Gao, Synthesis and characterization of silica nanoparticles with well-defined thermoresponsive PNIPAM via a combination of RAFT and click chemistry, ACS Appl. Mater. Interfaces. 3 (2011) 3215–3223. https://doi.org/10.1021/am2007189.

[90] W. Li, Y. Xu, Y. Zhou, W. Ma, S. Wang, Y. Dai, Silica nanoparticles functionalized via click chemistry and ATRP for enrichment of Pb(II) ion, Nanoscale Res. Lett. 7 (2012) 1. https://doi.org/10.1186/1556-276X-7-485.

[91] Y. Huang, T. Hou, X. Cao, S. Perrier, Y. Zhao, Synthesis of silica-polymer hybrids by combination of RAFT polymerization and azide-alkyne cycloaddition “click” reactions, Polym. Chem. 1 (2010) 1615–1623. https://doi.org/10.1039/c0py00165a.

[92] W. Yuan, F. Wang, Z. Chen, C. Gao, P. Liu, Y. Ding, S. Zhang, M. Yang, Efficient grafting of polypropylene onto silica nanoparticles and the properties of PP/PP-g-SiO2 nanocomposites, Polym. (United Kingdom). 151 (2018) 242–249. https://doi.org/10.1016/j.polymer.2018.07.060.

[93] W. Wei, Y. Zhao, B. Zhang, Y. Cui, X. Li, X. Fei, X. Liu, Silica/poly(styrene-alt-maleic anhydride) hybrid particles as a reactive toughener for epoxy resin, J. Appl. Polym. Sci. 137 (2020). https://doi.org/10.1002/app.48986.

[94] L. Tripaldi, E. Callone, M. D’Arienzo, S. Dirè, L. Giannini, S. Mascotto, A. Meyer, R. Scotti, L. Tadiello, B. Di Credico, Silica hairy nanoparticles: a promising material for self-assembling processes, Soft Matter. 17 (2021) 9434–9446. https://doi.org/10.1039/d1sm01085a.

[95] N.P. Truong, G.R. Jones, K.G.E. Bradford, D. Konkolewicz, A. Anastasaki, A comparison of RAFT and ATRP methods for controlled radical polymerization, Nat. Rev. Chem. (2021). https://doi.org/10.1038/s41570-021-00328-8.

[96] S.K. Ghosh, A. Böker, Self-Assembly of Nanoparticles in 2D and 3D: Recent Advances and Future Trends, Macromol. Chem. Phys. 220 (2019).

https://doi.org/10.1002/macp.201900196.

[97] N.J. Fernandes, H. Koerner, E.P. Giannelis, R.A. Vaia, Hairy Nanoparticle Assemblies as One-Component Functional Polymer Nanocomposites: Opportunities and Challenges, MRS Commun. 3 (2013) 13–29. https://doi.org/10.1557/mrc.2013.9.

[98] A.J. Chancellor, B.T. Seymour, B. Zhao, Characterizing Polymer-Grafted Nanoparticles: From Basic Defining Parameters to Behavior in Solvents and Self-Assembled Structures, Anal. Chem. (2019). https://doi.org/10.1021/acs.analchem.9b00707.

[99] A. Rungta, B. Natarajan, T. Neely, D. Dukes, L.S. Schadler, B.C. Benicewicz, Grafting bimodal polymer brushes on nanoparticles using controlled radical polymerization, Macromolecules. 45 (2012) 9303–9311. https://doi.org/10.1021/ma3018876.

[100] D. Zhao, M. Di Nicola, M.M. Khani, J. Jestin, B.C. Benicewicz, S.K. Kumar, Self-Assembly of Monodisperse versus Bidisperse Polymer-Grafted Nanoparticles, ACS Macro Lett. 5 (2016) 790–795. https://doi.org/10.1021/acsmacrolett.6b00349.

[101] P.G. de Gennes, Conformations of Polymers Attached to an Interface, Macromolecules. 13 (1980) 1069–1075. https://doi.org/10.1021/ma60077a009.

[102] S. Alexander, Adsorption of Chain Molecules With a Polar Head. a Scaling Description., J Phys. 38 (1977) 983–987. https://doi.org/10.1051/jphys:01977003808098300.

[103] M. Daoud, J.P. Cotton, Star Shaped Polymers: a Model for the Conformation and Its Concentration Dependence., J. Phys. Paris. 43 (1982) 531–538. https://doi.org/10.1051/jphys:01982004303053100.

[104] K. Ohno, T. Morinaga, S. Takeno, Y. Tsujii, T. Fukuda, Suspensions of silica particles grafted with concentrated polymer brush: Effects of graft chain length on brush layer thickness and colloidal crystallization, Macromolecules. 40 (2007) 9143–9150. https://doi.org/10.1021/ma071770z.

[105] D. Dukes, Y. Li, S. Lewis, B. Benicewicz, L. Schadler, S.K. Kumar, Conformational transitions of spherical polymer brushes: Synthesis, characterization, and theory,

Macromolecules. 43 (2010) 1564–1570. https://doi.org/10.1021/ma901228t.

[106] W.J. Brittain, S. Minko, A structural definition of polymer brushes, J. Polym. Sci. Part A Polym. Chem. 45 (2007) 3505–3512. https://doi.org/10.1002/pola.22180.

[107] D.W. Lee, B.R. Yoo, Advanced silica/polymer composites: Materials and applications, J. Ind. Eng. Chem. 38 (2016) 1–12. https://doi.org/10.1016/j.jiec.2016.04.016.

[108] S. Mallakpour, M. Naghdi, Polymer/SiO2 nanocomposites: Production and applications, Prog. Mater. Sci. 97 (2018) 409–447. https://doi.org/10.1016/j.pmatsci.2018.04.002.

[109] A.J. Crosby, J.Y. Lee, Polymer Nanocomposites: The “Nano” Effect on Mechanical Properties, Polym. Rev. 47 (2007) 217–229. https://doi.org/10.1080/15583720701271278.

[110] M. Maiti, M. Bhattacharya, A.K. Bhowmick, Elastomer Nanocomposites, Rubber Chem. Technol. 81 (2008) 384–469. https://doi.org/10.5254/1.3548215.

[111] Q. Xue, J. Sun, Electrical Conductivity and Percolation Behavior of Polymer Nanocomposites, in: Polym. Nanocomposites, Springer International Publishing, Cham, 2016: pp. 51–82. http://link.springer.com/10.1007/978-3-319-28238-1_3.

[112] N. Hamadneh, W.A. Khan, W.S. Khan, Polymer nanocomposites – synthesis techniques, classification and properties, Sci. Appl. Tailored Nanostructures. (2016) 50–67.

[113] G.A. Ozin, K. Hou, B. V. Lotsch, L. Cademartiri, D.P. Puzzo, F. Scotognella, A. Ghadimi, J. Thomson, Nanofabrication by self-assembly, Mater. Today. 12 (2009) 12–23. https://doi.org/10.1016/S1369-7021(09)70156-7.

[114] R.G. Nuzzo, D.L. Allara, Adsorption of Bifunctional Organic Disulfides on Gold Surfaces, J. Am. Chem. Soc. 105 (1983) 4481–4483. https://doi.org/10.1021/ja00351a063.

[115] I. Langmuir, K.B. Blodgett, Über einige neue Methoden zur Untersuchung von monomolekularen Filmen, Kolloid-Zeitschrift. (1935) 257–263. https://doi.org/10.1007/BF01428777.

[116] W.C. Bigelow, D.L. Pickett, W.A. Zisman, Oleophobic monolayers. I. Films adsorbed from solution in non-polar liquids, J. Colloid Sci. 1 (1946) 513–538. https://doi.org/10.1016/0095-

8522(46)90059-1.

[117] R.N. Perham, Self-assembly of biological macromolecules, Philos. Trans. R. Soc. Lond. B. Biol. Sci. 272 (1975) 123–136. https://doi.org/10.1098/rstb.1975.0075.

[118] G.M. Whitesides, B. Grzybowski, Self-assembly at all scales, Science (80-.). 295 (2002) 2418–2421. https://doi.org/10.1126/science.1070821.

[119] L. Cademartiri, K.J.M. Bishop, P.W. Snyder, G.A. Ozin, Using shape for self-assembly, Philosphical Trans. R. Soc. 370 (2012) 2824–2847.

[120] C. Yi, Y. Yang, B. Liu, J. He, B. Liu, Polymer-guided assembly of inorganic nanoparticles, Chem. Soc. Rev. 49 (2020) 465–508. https://doi.org/10.1039/c9cs00725c.

[121] K. Thorkelsson, P. Bai, T. Xu, Self-assembly and applications of anisotropic nanomaterials: A review, Nano Today. 10 (2015) 48–66. https://doi.org/10.1016/j.nantod.2014.12.005.

[122] N.R. Jana, Shape Effect in Nanoparticle Self-Assembly, Angew. Chemie. 116 (2004) 1562–1566. https://doi.org/10.1002/ange.200352260.

[123] X. Li, Z. Li, J. Shen, Z. Zheng, J. Liu, Role of a nanoparticle network in polymer mechanical reinforcement: Insights from molecular dynamics simulations, Phys. Chem. Chem. Phys. 23 (2021) 21797–21807. https://doi.org/10.1039/d1cp03153h.

[124] N. Jouault, D. Zhao, S.K. Kumar, Role of casting solvent on nanoparticle dispersion in polymer nanocomposites, Macromolecules. 47 (2014) 5246–5255. https://doi.org/10.1021/ma500619g.

[125] P. Lepcio, F. Ondreas, K. Zarybnicka, M. Zboncak, O. Caha, J. Jancar, Bulk polymer nanocomposites with preparation protocol governed nanostructure: The origin and properties of aggregates and polymer bound clusters, Soft Matter. 14 (2018) 2094–2103. https://doi.org/10.1039/c8sm00150b.

[126] F. Ondreas, P. Lepcio, M. Zboncak, K. Zarybnicka, L.E. Govaert, J. Jancar, Effect of Nanoparticle Organization on Molecular Mobility and Mechanical Properties of Polymer Nanocomposites, Macromolecules. 52 (2019) 6250–6259.

https://doi.org/10.1021/acs.macromol.9b01197.

[127] A. Bouty, L. Petitjean, J. Chatard, R. Matmour, C. Degrandcourt, R. Schweins, F. Meneau, P. Kwaśniewski, F. Boué, M. Couty, J. Jestin, Interplay between polymer chain conformation and nanoparticle assembly in model industrial silica/rubber nanocomposites, Faraday Discuss. 186 (2016) 325–343. https://doi.org/10.1039/c5fd00130g.

[128] S. Cheng, G.S. Grest, Dispersing Nanoparticles in a Polymer Film via Solvent Evaporation, ACS Macro Lett. 5 (2016) 694–698. https://doi.org/10.1021/acsmacrolett.6b00263.

[129] P. Akcora, H. Liu, S.K. Kumar, J. Moll, Y. Li, B.C. Benicewicz, L.S. Schadler, D. Acehan, A.Z. Panagiotopoulos, V. Pryamitsyn, V. Ganesan, J. Ilavsky, P. Thiyagarajan, R.H. Colby, J.F. Douglas, Anisotropic self-assembly of spherical polymer-grafted nanoparticles, Nat. Mater. 8 (2009) 354–359. https://doi.org/10.1038/nmat2404.

[130] S.K. Kumar, N. Jouault, B. Benicewicz, T. Neely, Nanocomposites with polymer grafted nanoparticles, Macromolecules. 46 (2013) 3199–3214. https://doi.org/10.1021/ma4001385.

[131] S.J. Park, S. Kim, D. Yong, Y. Choe, J. Bang, J.U. Kim, Interactions between brush-grafted nanoparticles within chemically identical homopolymers: The effect of brush polydispersity, Soft Matter. 14 (2018) 1026–1042. https://doi.org/10.1039/c7sm02483e.

[132] W.R. Lenart, M.J.A. Hore, Structure–property relationships of polymer-grafted nanospheres for designing advanced nanocomposites, Nano-Structures and Nano-Objects. 16 (2018) 428–440. https://doi.org/10.1016/j.nanoso.2017.11.005.

[133] T.B. Martin, K.I.S. Mongcopa, R. Ashkar, P. Butler, R. Krishnamoorti, A. Jayaraman, Wetting − Dewetting and Dispersion − Aggregation Transitions Are Distinct for Polymer Grafted Nanoparticles in Chemically Dissimilar Polymer Matrix, (2015). https://doi.org/10.1021/jacs.5b05291.

[134] D. Sunday, J. Ilavsky, D.L. Green, A phase diagram for polymer-grafted nanoparticles in homopolymer matrices, Macromolecules. 45 (2012) 4007–4011. https://doi.org/10.1021/ma300438g.

[135] P.F. Green, The structure of chain end-grafted nanoparticle/homopolymer nanocomposites, Soft Matter. 7 (2011) 7914–7926. https://doi.org/10.1039/c1sm05076a.

[136] C. Yi, S. Zhang, K.T. Webb, Z. Nie, Anisotropic self-assembly of hairy inorganic nanoparticles, Acc. Chem. Res. 50 (2017) 12–21. https://doi.org/10.1021/acs.accounts.6b00343.

[137] D. Maillard, S.K. Kumar, A. Rungta, B.C. Benicewicz, R.E. Prud'Homme, Polymer-Grafted-Nanoparticle surfactants, Nano Lett. 11 (2011) 4569–4573. https://doi.org/10.1021/nl202651u.

[138] C. Chevigny, F. Dalmas, E. Di Cola, D. Gigmes, D. Bertin, F. Boué, J. Jestin, Polymer-grafted-nanoparticles nanocomposites: Dispersion, grafted chain conformation, and rheological behavior, Macromolecules. 44 (2011) 122–133. https://doi.org/10.1021/ma101332s.

[139] P. Akcora, S.K. Kumar, V. García Sakai, Y. Li, B.C. Benicewicz, L.S. Schadler, Segmental dynamics in PMMA-grafted nanoparticle composites, Macromolecules. 43 (2010) 8275–8281. https://doi.org/10.1021/ma101240j.

[140] D.L. Green, J. Mewis, Connecting the wetting and rheological behaviors of poly(dimethylsiloxane)- grafted silica spheres in poly(dimethylsiloxane) melts, Langmuir. 22 (2006) 9546–9553. https://doi.org/10.1021/la061136z.

[141] M. Bonnevide, A.M. Jimenez, D. Dhara, T.N.T. Phan, N. Malicki, Z.M. Abbas, B. Benicewicz, S.K. Kumar, M. Couty, D. Gigmes, J. Jestin, Morphologies of Polyisoprene-Grafted Silica Nanoparticles in Model Elastomers, Macromolecules. 52 (2019) 7638–7645. https://doi.org/10.1021/acs.macromol.9b01479.

[142] D. Dhara, M.A. Rahman, Z. Abbas, E. Ruzicka, B. Benicewicz, S.K. Kumar, Melt State Reinforcement of Polyisoprene by Silica Nanoparticles Grafted with Polyisoprene, ACS Macro Lett. (2022) 1325–1330. https://doi.org/10.1021/acsmacrolett.2c00507.

[143] K. Bornani, M.A. Rahman, B. Benicewicz, S. Kumar, L. Schadler, Using Nanofiller

Assemblies to Control the Crystallization Kinetics of High-Density Polyethylene, Macromolecules. 54 (2021) 5673–5682. https://doi.org/10.1021/acs.macromol.1c00341.

[144] A.K. Boal, F. Ilhan, J.E. Derouchey, T. Thurn-Albrecht, T.P. Russell, V.M. Rotello, Self-assembly of nanoparticles into structured spherical and network aggregates, Nature. 404 (2000) 746–748. https://doi.org/10.1038/35008037.

[145] B. Natarajan, T. Neely, A. Rungta, B.C. Benicewicz, L.S. Schadler, Thermomechanical properties of bimodal brush modified nanoparticle composites, Macromolecules. 46 (2013) 4909–4918. https://doi.org/10.1021/ma400553c.

[146] T.B. Martin, A. Jayaraman, Identifying the ideal characteristics of the grafted polymer chain length distribution for maximizing dispersion of polymer grafted nanoparticles in a polymer matrix, Macromolecules. 46 (2013) 9144–9150. https://doi.org/10.1021/ma401763y.

[147] S. Tang, T.L. Fox, T.Y. Lo, J.M. Horton, R.M. Ho, B. Zhao, P.L. Stewart, L. Zhu, Environmentally responsive self-assembly of mixed poly(tert-butyl acrylate)-polystyrene brush-grafted silica nanoparticles in selective polymer matrices, Soft Matter. 11 (2015) 5501–5512. https://doi.org/10.1039/c5sm00193e.

Declaration of interests

☒ The authors declare that they have no known competing financial interests or personal relationships that could have appeared to influence the work reported in this paper.

☐The authors declare the following financial interests/personal relationships which may be considered as potential competing interests: